

**Effect of Heating and Cooling Strips on
Boundary Layer Stability of Nozzles and Test
Sections of Supersonic Wind Tunnels**

A Thesis

Presented for the

Master of Science

Degree

The University of Tennessee, Knoxville

William Scott Meredith

December 1994

THE UNIVERSITY OF CHICAGO PRESS

1997

1998

1999

2000



Dedication

**This thesis is dedicated to my parents
Mr. Bob L. Meredith and Mrs. Patricia C. Meredith
without whose support this would not have
been possible.**

Acknowledgments

I would like to express my sincere appreciation to Dr. Ching F. Lo for his support and suggestions during the completion of this thesis. I would also like to thank my committee members, Dr. Ahmad D. Vakili and Dr. Frank G. Collins, for their time and assistance.

Also my appreciation is extended to Mr. Robert Lafrance for his help in learning the computer codes used in this project and to Mr. Lyndell S. King for his assistance in running the computer codes.

This work was partially supported by NASA Grant No. NAG 2-881.

Abstract

It has been shown in the past that the turbulent boundary layer of supersonic wind tunnel nozzle and test section walls affects adversely the transition Reynolds number on models in the wind tunnel. If the boundary layer of the nozzle and test section is kept laminar, the boundary layer disturbance can be eliminated. Two different computational methods are used to study the effects of heating and cooling strips on the stability of the laminar boundary layer of the nozzles and test section walls of the Laminar Flow Supersonic Wind Tunnel (LFSWT) and the 1/8 scale of the LFSWT called the Proof of Concept (PoC) Supersonic Wind Tunnel at NASA Ames Research Center. The first method used is the Stability Modifiers Method, which examines the second derivative of velocity near the wall to study stability of the boundary layer. The second method is the e^N Method, where e^N is an exponential function of N and N is known as the N Factor. The N Factor value is used to investigate boundary layer stability. Results of this study indicate that heating applied upstream of the location of instability on-set can enhance boundary layer stability. Applying cooling near the point of the on-set of instability and downstream increases boundary layer stability. When cooling is applied upstream and heating is applied downstream of the on-set points of instability, the boundary layer becomes more destabilized. The effects of heating and cooling are predicted by the methods of the present study and can be utilized to model the actual temperature distribution of experiments.

Table of Contents

Chapter	Page
1 Introduction.....	1
1.1 Background.....	1
1.2 Wind Tunnel Disturbances.....	2
1.3 Approach.....	4
2 Study of Boundary Layer Stability Using Stability Modifier Method.....	6
2.1 Stability Modifier Method.....	6
2.2 Boundary Layer Code.....	7
2.3 Results Obtained for the PoC Supersonic Wind Tunnel.....	8
2.4 Summary of Results.....	18
3 Study of Boundary Layer Stability Using e^N Method.....	23
3.1 Summary of Compressible Linear Stability Theory and e^N Method.....	23
3.2 Description of e^{Malik} Code.....	24
3.3 Results Obtained for the PoC Wind Tunnel.....	25
3.4 LFSWT Results	34
3.5 Summary of Results.....	34
4 Conclusions and Recommendations.....	39
4.1 Conclusions.....	39
4.2 Recommendations.....	41

List of References.....	42
Bibliography.....	45
Vita.....	47

List of Figures

Figure	Page
1.1 Skin-friction coefficient for Laminar and Turbulent Flow.....	2
1.2 Wind Tunnel Disturbances.....	3
2.1 Growth of Boundary Layer for the Adiabatic and Strip Heating Case. The location of the Heating Strip ($2.86 \leq X/H \leq 3.73$) on the nozzle wall is shown in bold.....	9
2.2 Growth of Boundary Layer for the Adiabatic and Strip Cooling Case. The location of the Cooling Strip ($2.86 \leq X/H \leq 3.73$) on the nozzle wall is shown in bold.....	10
2.3 Comparison for the first derivative of temperature profiles at $X/H=5.23$ with the Heating/Cooling Strip at $2.86 \leq X/H \leq 3.73$	11
2.4 Comparison of the second derivative of velocity profiles at $X/H=5.23$ with the Heating/Cooling Strip at $2.86 \leq X/H \leq 3.73$	13
2.5 Comparison for the first derivative of temperature profiles at $X/H=9.23$ with the Heating/Cooling Strip at $2.86 \leq X/H \leq 3.73$	14
2.6 Comparison of the second derivative of velocity profiles at $X/H=9.23$ with the Heating/Cooling Strip at $2.86 \leq X/H \leq 3.73$	15
2.7 Growth of Boundary Layer for the Adiabatic and Strip Heating Case. The location of the Heating Strip ($5.61 \leq X/H \leq 6.41$) on the nozzle wall is shown in bold.....	16
2.8 Growth of Boundary Layer for the Adiabatic and Strip Cooling Case. The location of the Cooling Strip ($5.61 \leq X/H \leq 6.41$) on the nozzle wall is shown in bold.....	17
2.9 Comparison of the first derivative of temperature profiles at $X/H=5.23$ with the Heating/Cooling Strip at $5.61 \leq X/H \leq 6.41$	19
2.10 Comparison of the second derivative of velocity profiles at $X/H=5.23$ with the Heating/Cooling Strip at $5.61 \leq X/H \leq 6.41$	20

2.11	Comparison for the first derivative of temperature profiles at $X/H=9.23$ with the Heating/Cooling Strip at $5.61 \leq X/H \leq 6.41$	21
2.12	Comparison of the second derivative of velocity profiles at $X/H=9.23$ with the Heating/Cooling Strip at $5.61 \leq X/H \leq 6.41$	22
3.1	N Factor Growth with the Heating/Cooling Strip located at $0.00 \leq X/H \leq 0.84$ for a disturbance frequency of 14 kHz.....	26
3.2	N Factor Growth with the Heating/Cooling Strip located at $0.88 \leq X/H \leq 1.85$ for a disturbance frequency of 14 kHz.....	28
3.3	N Factor Growth with the Heating/Cooling Strip located at $1.93 \leq X/H \leq 2.78$ for a disturbance frequency of 14 kHz.....	29
3.4	N Factor Growth with the Heating/Cooling Strip located at $2.86 \leq X/H \leq 3.73$ for a disturbance frequency of 14 kHz.....	30
3.5	N Factor Growth with the Heating/Cooling Strip located at $3.80 \leq X/H \leq 4.59$ for a disturbance frequency of 14 kHz.....	31
3.6	N Factor Growth with the Heating/Cooling Strip located at $4.67 \leq X/H \leq 5.54$ for a disturbance frequency of 14 kHz.....	32
3.7	N Factor Growth with the Heating/Cooling Strip located at $5.61 \leq X/H \leq 6.41$ for a disturbance frequency of 14 kHz.....	33
3.8	Comparison of Boundary Layer growth for the Adiabatic case and the case where the Heating Strip is located at $0.48 \leq X/H \leq 1.23$ on the nozzle of the LFSWT.....	35
3.9	Comparison of Boundary Layer growth for the Adiabatic case and the case where the Cooling Strip is located at $0.48 \leq X/H \leq 1.23$ on the nozzle of the LFSWT.....	36
3.10	N Factor growth for the Adiabatic case, case where the Heating Strip is located at $0.48 \leq X/H \leq 1.23$ and the case where the Cooling Strip is located at $0.48 \leq X/H \leq 1.23$ for the LFSWT. Frequency = 3000 Hz.....	37

Nomenclature

f	Dimensional disturbance frequency
H	Test section height
p	Pressure
\tilde{p}	Sound disturbance
\bar{p}	Mean pressure
\hat{p}	Disturbance Pressure
T	Temperature
\tilde{T}	Entropy fluctuations
t	Time
u	Velocity in flow direction
\tilde{u}	Turbulence
\bar{u}	Mean velocity in flow direction
\hat{u}	Disturbance velocity in flow direction
v	Velocity normal to flow direction
β	Z wave number
α	X wave number
μ	Coefficient of viscosity
ρ	Density
ω	Frequency of disturbance

Subscripts

e Edge of boundary layer

w Wall

Chapter 1

Introduction

1.1 Background

Viscous drag will account for a major portion of the total drag for aircraft such as the High-Speed Civil Transport (HSCT). Since skin-friction can be an order of magnitude higher for turbulent flow than for laminar flow, as seen in Figure 1.1, laminar flow control offers a way to reduce the drag on aircraft like the HSCT and thus to increase range, payload, fuel load, etc. of these aircraft. Because modern supersonic wind tunnels produce disturbances, development of Quiet Supersonic Wind Tunnels is important to study laminar flow control techniques. One of the major disturbances in these wind tunnels is noise radiated from the turbulent boundary layer on the nozzle and test section walls. If the boundary layer could be kept laminar, this type of disturbance would be eliminated. The above considerations and the support of the NASA F-16 XL test aircraft in research of Supersonic Laminar Flow Control are the reasons behind the Quiet Wind Tunnel Development at NASA Ames Research Center. Its purpose is to develop the Laminar Flow Supersonic Wind Tunnel (LFSWT) and a 1/8 scale of the LFSWT called the Proof of Concept (PoC) Supersonic Wind Tunnel (Reference 1). The test section of the LFSWT has cross sectional dimensions of 8 X 16 inches. Both the LFSWT and the PoC have two-

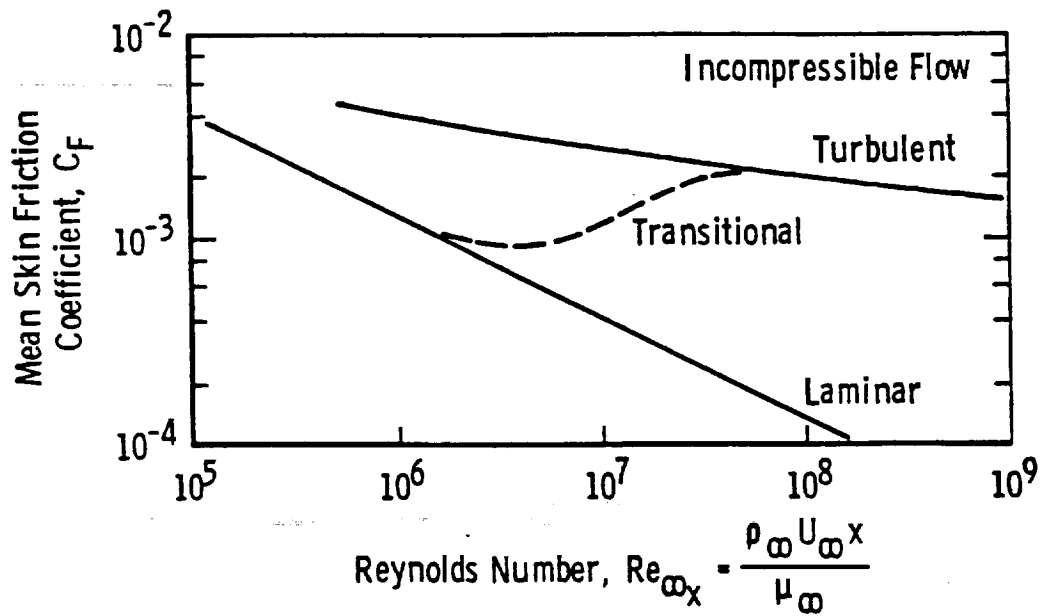


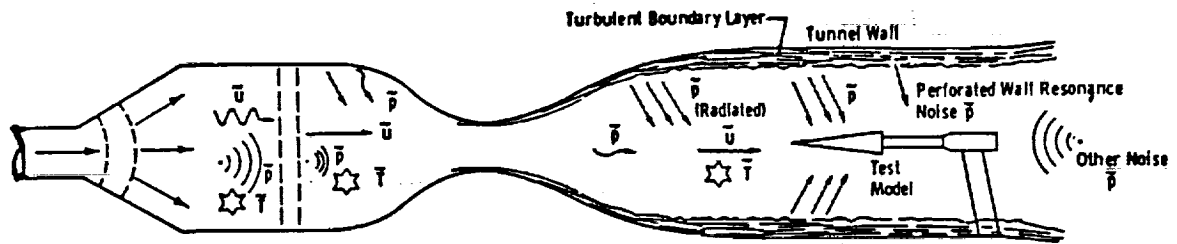
Figure 1.1 Skin-friction coefficient for Laminar and Turbulent Flow (From Reference 2)

dimensional nozzles.

1.2 Wind Tunnel Disturbances

In 1953 Kovasznay theorized on the modes of disturbances in wind tunnels, vorticity (free stream turbulence), entropy mode (temperature spottiness) and sound waves (Reference 3). Vorticity fluctuations and entropy fluctuations are convected to the test section along streamlines which can be traced back upstream to the stilling chamber and beyond, and sound wave disturbance can radiate across streamlines.

Thus, these disturbances can originate from a variety of locations. Figure 1.2 shows



Vorticity (Turbulence - Velocity Fluctuations), \tilde{u}
 Acoustic Sound (Pressure Fluctuations), \tilde{p}
 Entropy Fluctuations (Temperature Spottyness), \tilde{T}

Mach Number Range	Type Disturbance	Effect on Transition
Subsonic $M_\infty \leq 0.6$	Velocity Fluctuations, \tilde{u} Acoustic Noise, \tilde{p} Temperature Fluctuations, \tilde{T}	• Usually Dominant • Can be Dominant Negligible
Transonic $0.6 \leq M_\infty \leq 1.3$	Velocity Fluctuations, \tilde{u} Acoustic Noise, \tilde{p} Temperature Fluctuations, \tilde{T}	• Can be Dominant • Usually Dominant Negligible
Supersonic $1.3 \leq M_\infty \leq 6$	Velocity Fluctuations, \tilde{u} Radiated Noise, \tilde{p} Temperature Fluctuations, \tilde{T}	Usually Negligible • Usually Dominant Usually Negligible
Hypersonic $6 \leq M_\infty \leq 15$	Velocity Fluctuations, \tilde{u} Radiated Noise, \tilde{p} Temperature Fluctuations, \tilde{T}	Usually Negligible • Usually Dominant Could be Significant

Figure 1.2 Wind Tunnel Disturbances (From Reference 9)

all the possible locations of disturbances in a wind tunnel and the dominance of such disturbances for different Mach number ranges. In the supersonic Mach number range, the speed regime of aircraft like the HSCT and the F-16 XL, the disturbance that usually dominates transition on the test model is sound disturbance and, more specifically, the radiated noise from the turbulent boundary layer on the nozzle wall and test section, as seen in the Table of Figure 1.2. This was deduced by Laufer (Reference 4) and shown conclusively by Pate and Schueler (Reference 5). These

revelations about sound disturbance by Laufer, Pate, Schueler, and others led to the work in the development of Quiet Wind Tunnels at NASA Langley Research Center, which is concentrating on Mach numbers from high supersonic to hypersonic (References 6-8).

1.3 Approach

It has been shown that the turbulent boundary layer on nozzle and test section walls of a supersonic wind tunnel has an adverse effect on the transition Reynolds number on models in the wind tunnel (References 4 and 5). In this thesis, a computational study will use two different methods to determine the stability of the boundary layer on the nozzles and test section walls by examining the effects of heating and cooling strips placed at various locations in the Proof of Concept (PoC) Supersonic Wind Tunnel and the Laminar Flow Supersonic Wind Tunnel (LFSWT) of NASA Ames Research Center.

There are several recent studies on the effect of heating and cooling on boundary layer stability. Demetriades has experimentally studied the effects of heating and cooling on the stability of the boundary layer of supersonic wind tunnel nozzles (References 10-11). Masad and Nayfeh have computed the effects of cooling and heating strips on the stability of the boundary layer for a flat plate at subsonic Mach numbers (Reference 12). This present study is an extension of Lafrance's

computations on cooling and heating effects on boundary layer stability for flat plates and for the PoC nozzle and test section at a supersonic Mach number (Reference 13).

The first method used is the Stability Modifiers Method (Reference 14). This method consists of examining the second derivative of velocity near the wall; the more negative this term is near the wall, the more stable the laminar boundary layer is. The term that affects the second derivative of velocity (in our case the first derivative of temperature) is obtained for all the different cases by the boundary layer code developed by Harris and Blanchard (Reference 15). This method and its results will be discussed in more detail for the PoC Wind Tunnel in Chapter 2 of this study.

The second method used to study the effect of heating and cooling strips on the stability of the boundary layer of the PoC wind tunnel and the LFSWT is the e^N Method. In this method the exponent of e^N , known as the N Factor, is obtained and gives an indication of the Tollmien-Schlichting instability of the boundary layer of the nozzle and test section walls. When external disturbances are small, N Factor values between 9 and 11 give a rough estimate of the location of transition. The N Factors for the various cases are obtained from a spatial compressible linear stability code called the e^{Malik} code (Reference 16). The e^{Malik} code also uses output from the boundary layer code developed by Harris and Blanchard described above (Reference 15).

Chapter 2

Study of Boundary Layer Stability Using Stability Modifier Method

2.1 Stability Modifier Method

The Stability Modifier Method (References 14 and 18) examines the second derivative of velocity as a means for determining the stability of a laminar boundary layer. The more negative the value of the second derivative near the wall, the more stable the boundary layer is. The factors that affect the second derivative of velocity, called stability modifiers, can be seen in the two-dimensional boundary layer momentum equation:

$$\mu_w \frac{\partial^2 u}{\partial y^2} = \left(\rho v_w - \frac{d\mu}{dT} \frac{\partial T}{\partial y} \right) \frac{\partial u}{\partial y} + \frac{dp}{dx} \quad (2.1)$$

Using the above equation, one can select several means of making the laminar boundary layer more stable. Favorable pressure gradients $\left(\frac{dp}{dx} < 0 \right)$ and the addition of suction ($v_w < 0$) to the boundary layer are two methods of improving stability of the boundary layer. Another way of improving stability is with the $\frac{\partial T}{\partial y}$ term. Since

for air the $\frac{d\mu}{dT}$ term is positive, the $\frac{\partial T}{\partial y}$ term must also be positive in order to make the second derivative of velocity $\left(\frac{\partial^2 u}{\partial y^2}\right)$ more negative. This means that the wall surface temperature must be cool relative to the boundary layer temperature.

This chapter examines wall temperature effects on the stability of the boundary layer. The Stability Modifier Method described above is used to investigate how wall temperature affects stability and, more specifically, how the $\frac{\partial T}{\partial y}$ term affects the $\frac{\partial^2 u}{\partial y^2}$ term.

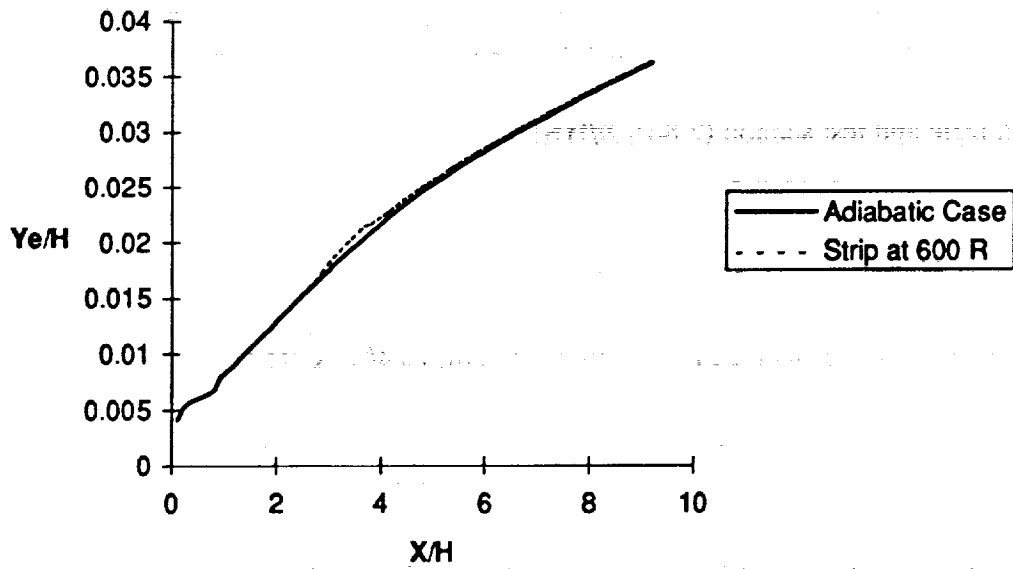
2.2 Boundary Layer Code

A boundary layer code developed by Harris and Blanchard (Reference 2) is used to obtain the values of $\frac{\partial T}{\partial y}$ and $\frac{\partial^2 u}{\partial y^2}$ for different cases considered. This code is capable of solving laminar, transitional, or turbulent perfect-gas compressible boundary layer equations for either axisymmetric or two-dimensional flows. The code, written in FORTRAN, uses a finite-difference method for solving the boundary layer equations. The present study uses this code to solve the laminar boundary layer equations.

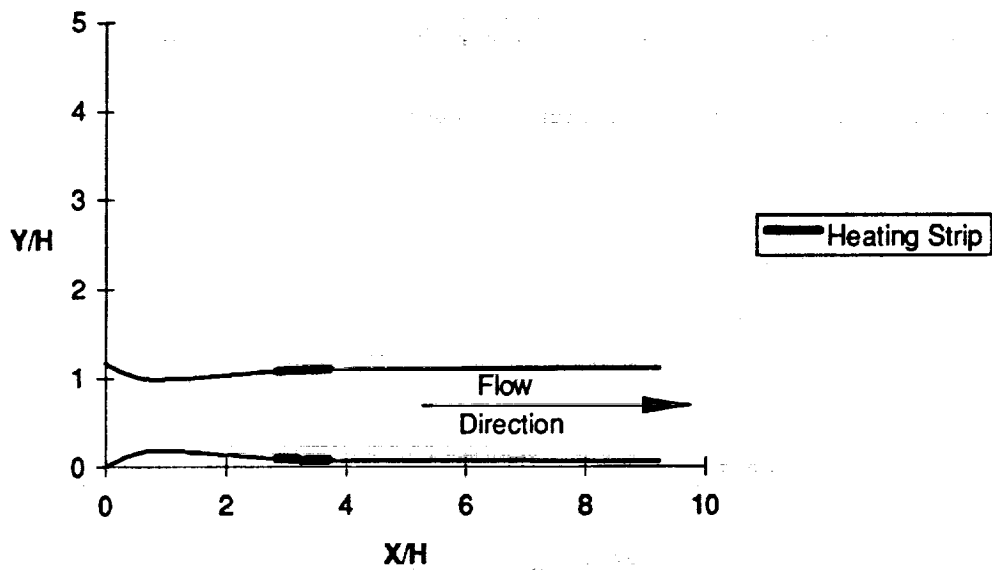
2.3 Results Obtained for the PoC Supersonic Wind Tunnel

In the first case a one-inch heater strip at 600°R is placed on the wall of the nozzle and test section ($2.86 \leq X/H \leq 3.73$) of the Proof of Concept (PoC) Wind Tunnel, as seen in Figure 2.1, where H is test section height, which is one inch for the PoC supersonic wind tunnel. The second case employs a cooling strip of the same length at 400°R located in the same locations ($2.86 \leq X/H \leq 3.73$) as the heating strip in case one, as seen in Figure 2.2. These two cases are compared to the adiabatic case for the PoC nozzle and test section in which the wall temperature is approximately 500°R . In all cases the stagnation pressure is 10 psia, the stagnation temperature is 530°R , and the test section Mach Number is 1.6. The heating strip causes the boundary layer to become thicker near the location of the heating strip as seen in Figure 2.1, and the cooling strip causes the boundary layer to become thinner near the location of the cooling strip, as seen in Figure 2.2.

A comparison of the temperature gradient, the first derivative of temperature, $\left(\frac{\partial T}{\partial y}\right)$ profiles at the $X/H = 5.23$ where the heating and cooling strips are located approximately 1.50 non-dimensional units upstream is shown along with the adiabatic case in Figure 2.3. From this figure it can be seen that the first derivative of temperature $\left(\frac{\partial T}{\partial y}\right)$ is positive near the wall in the case involving the heating strip because heat is applied upstream and the wall surface temperature is cool relative to the boundary layer temperature. The heat energy transfers out of the

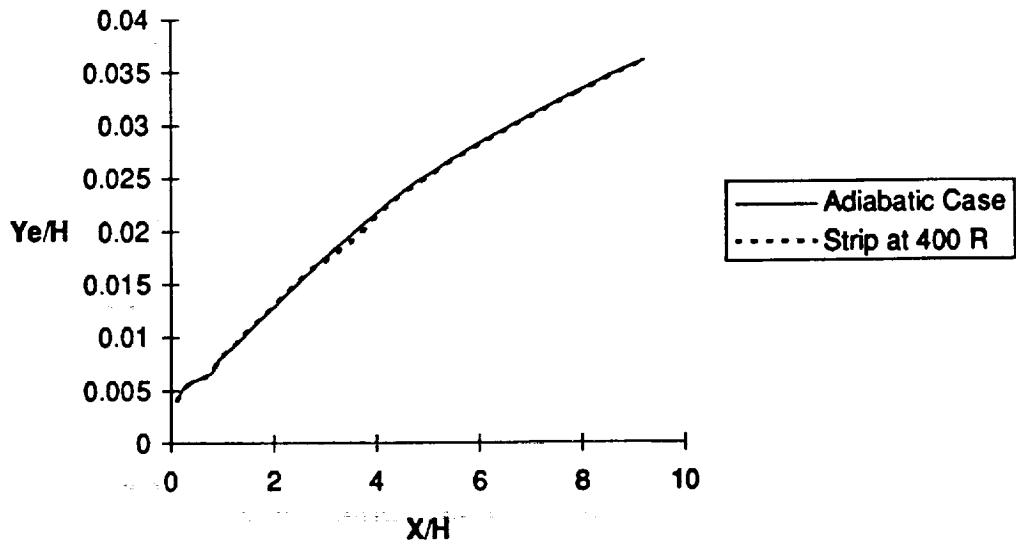


(a) Boundary Layer Growth

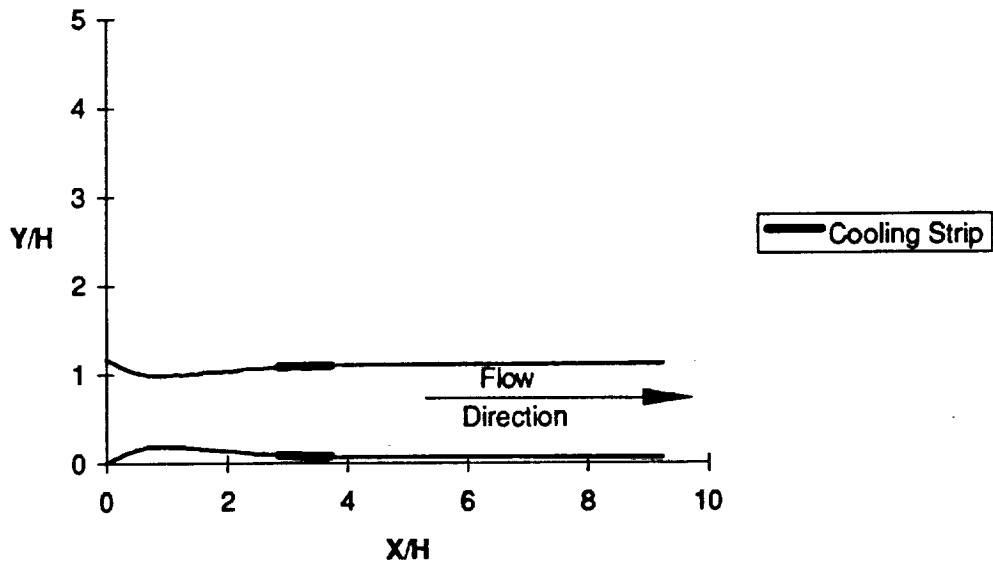


(b) PoC Nozzle and Test Section Geometry

Figure 2.1 Growth of Boundary Layer for the Adiabatic and Strip Heating Case. The location of the Heating Strip ($2.86 \leq X/H \leq 3.73$) on the nozzle wall is shown in bold

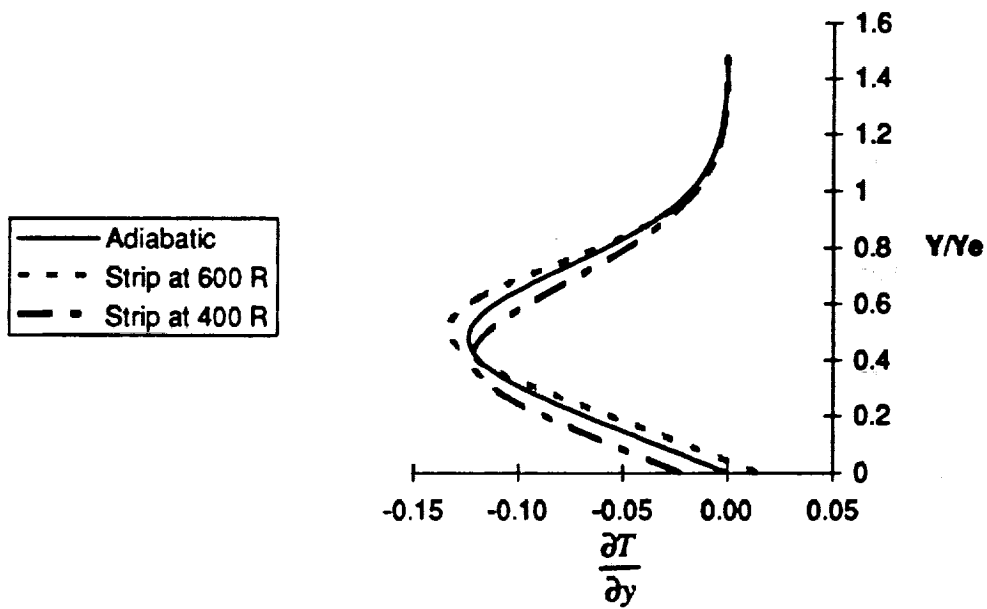


(a) Boundary Layer Growth

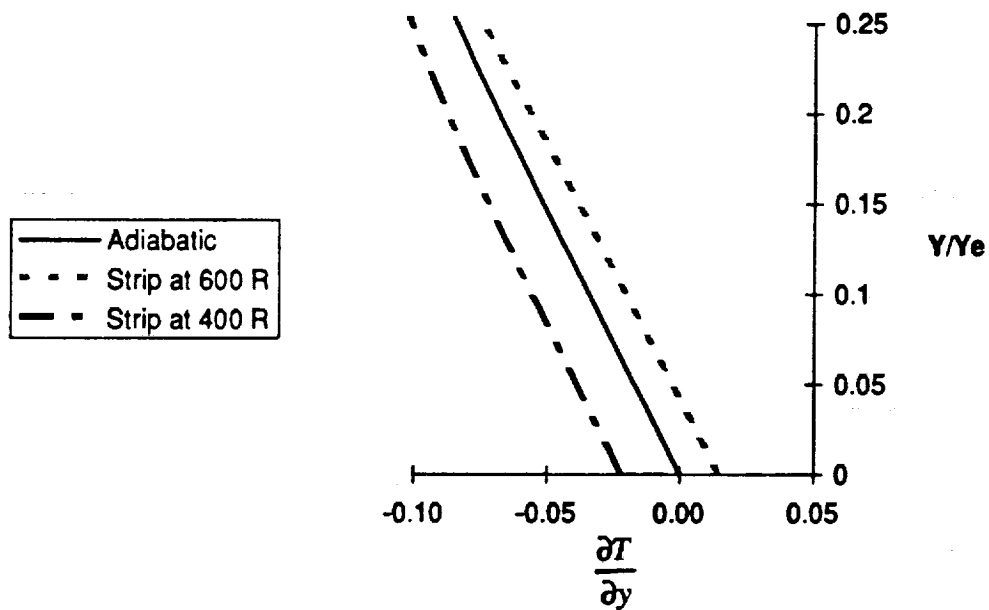


(b) PoC Nozzle and Test Section

Figure 2.2 Growth of Boundary Layer for the Adiabatic and Strip Cooling Case. The location of the Cooling Strip ($2.86 \leq X/H \leq 3.73$) on the nozzle wall is shown in bold



(a)



(b) Enlarged view near the wall

Figure 2.3 Comparison of the first derivative of temperature profiles at $X/H = 5.23$ with the Heating/Cooling Strip at $2.86 \leq X/H \leq 3.73$

boundary layer. The case where the cooling is applied has negative values of the first derivative of temperature $\left(\frac{\partial T}{\partial y}\right)$ near the wall. The second derivative of velocity $\left(\frac{\partial^2 u}{\partial y^2}\right)$ obtained from Figure 2.4 is the smallest value of all the cases when the heating strip is used, since the first derivative of temperature $\left(\frac{\partial T}{\partial y}\right)$ affects the second derivative of velocity profile at $X/H = 5.23$ along the nozzle. The largest value of $\left(\frac{\partial^2 u}{\partial y^2}\right)$ is obtained when the cooling strip is applied, (Figure 2.4). The first derivative of temperature $\left(\frac{\partial T}{\partial y}\right)$ and the second derivative of velocity $\left(\frac{\partial^2 u}{\partial y^2}\right)$ profiles are also obtained at $X/H = 9.23$ for the same cases as shown in Figures 2.5 and 2.6 respectively. The effect of the heating and cooling strips is not as great at $X/H=9.23$ as at $X/H = 5.23$ although the trend is similar.

The above procedure is then followed at a different location. A heating strip is placed at location $5.61 \leq X/H \leq 6.41$ as seen in Figure 2.7. In this Figure the boundary becomes thicker near the heating strip as it does at $2.86 \leq X/H \leq 3.73$. A cooling strip at $5.61 \leq X/H \leq 6.41$ causes the boundary layer to become thinner near the location of the cooling strip as seen in Figure 2.8. Comparisons of the first derivative of temperature and the second derivative of velocity profiles at $X/H = 5.23$, approximately four-tenths of a non-dimensional unit upstream of the heating /cooling

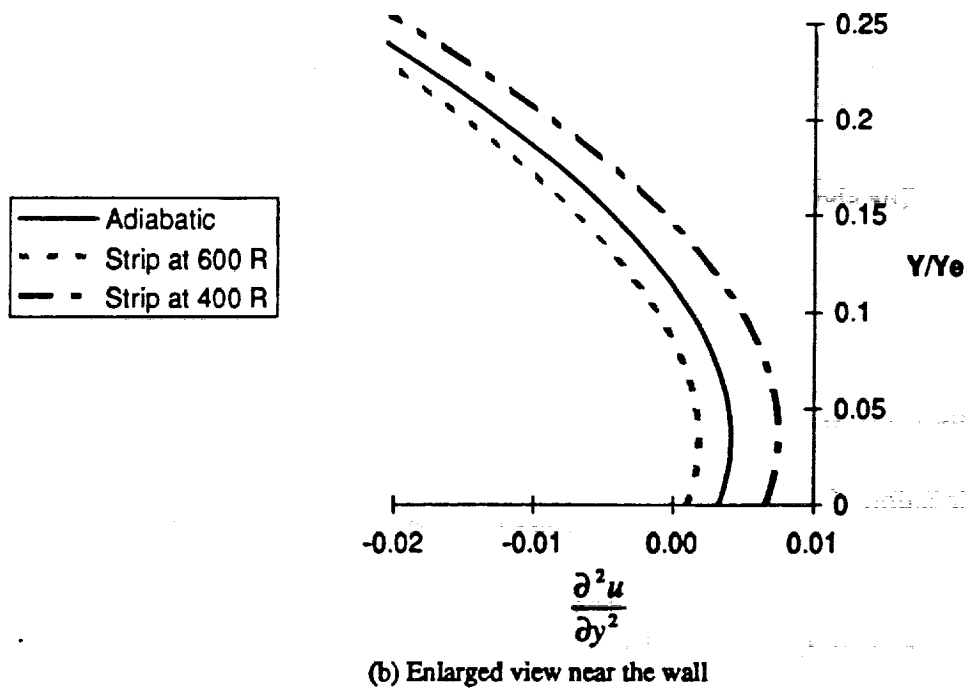
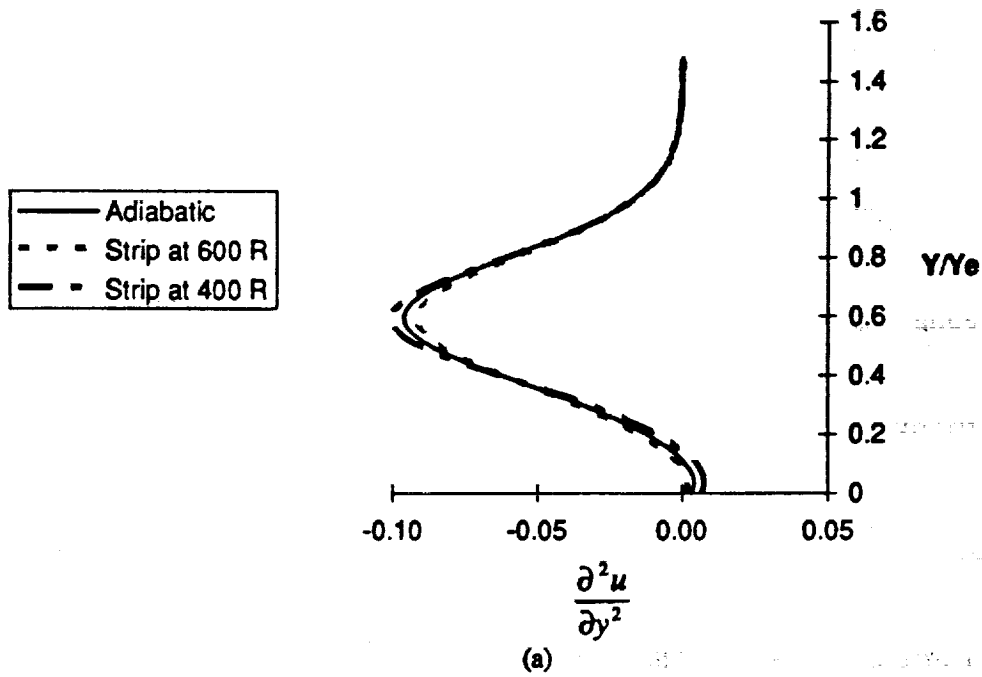
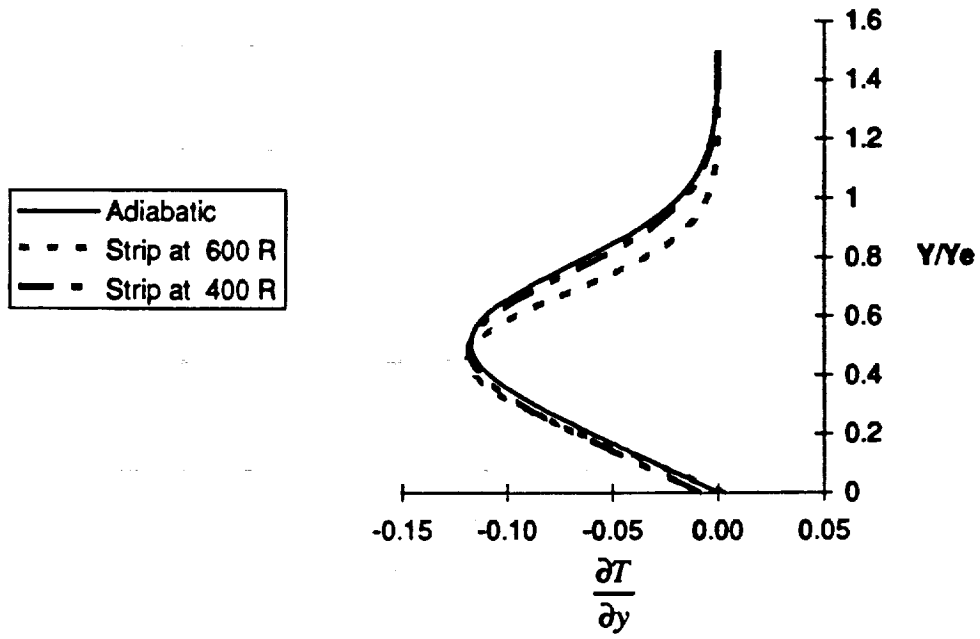
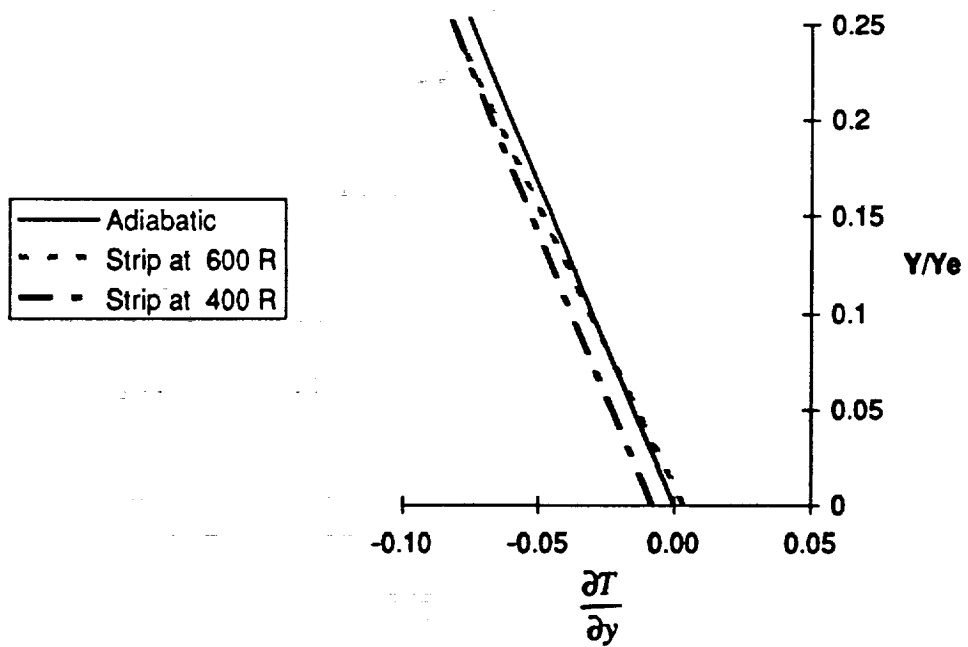


Figure 2.4 Comparison of the second derivative of velocity profiles at $X/H = 5.23$ with the Heating/Cooling Strip at $2.86 \leq X/H \leq 3.73$



(a)



(b) Enlarged view near the wall

Figure 2.5

Comparison of the first derivative of temperature profiles at $X/H = 9.23$ with the Heating/Cooling Strip at $2.86 \leq X/H \leq 3.73$

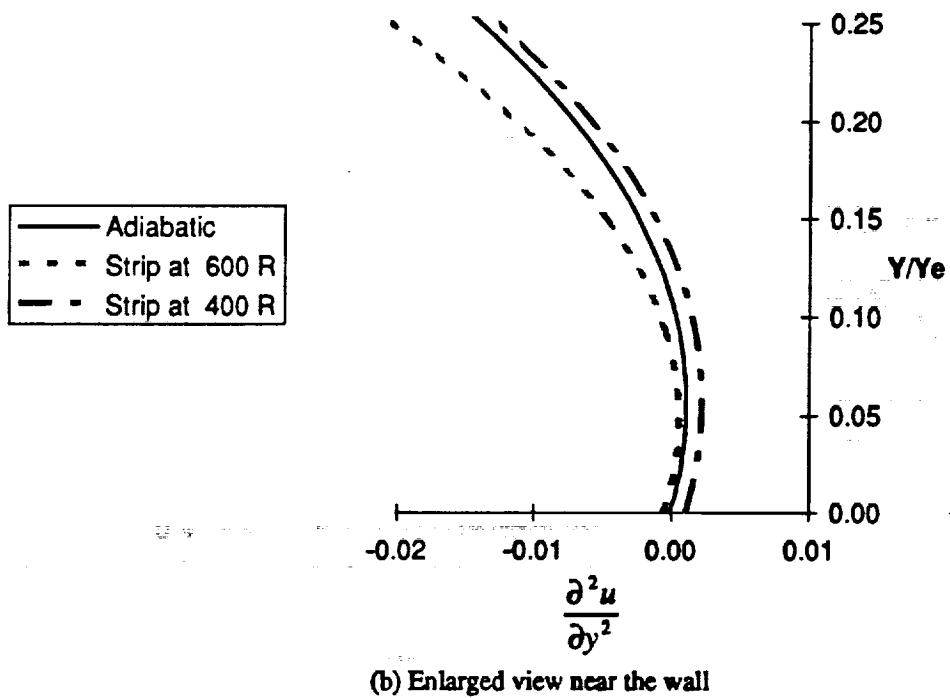
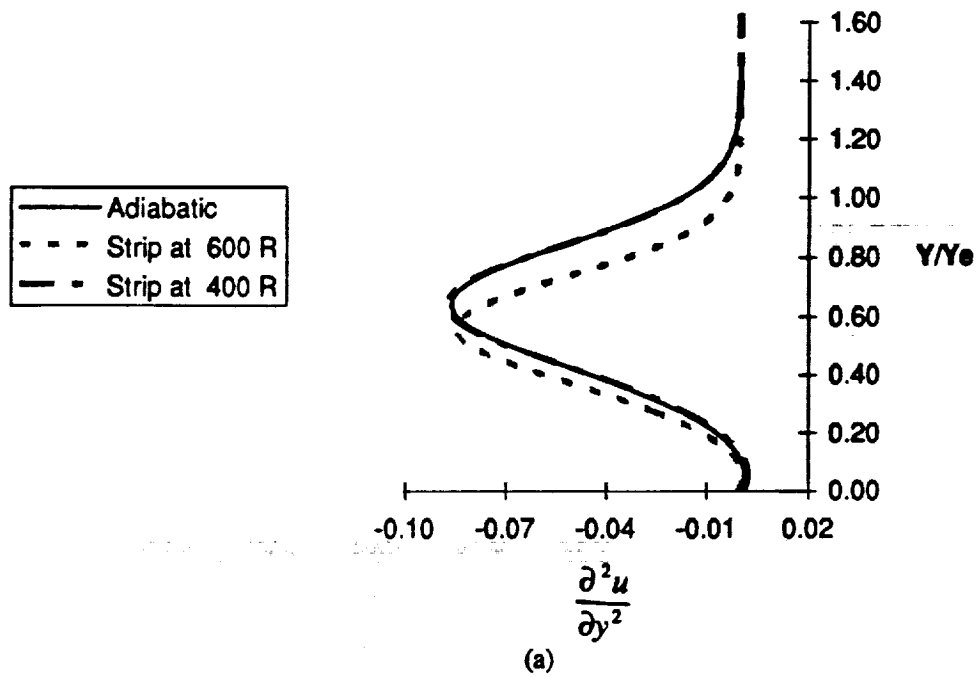
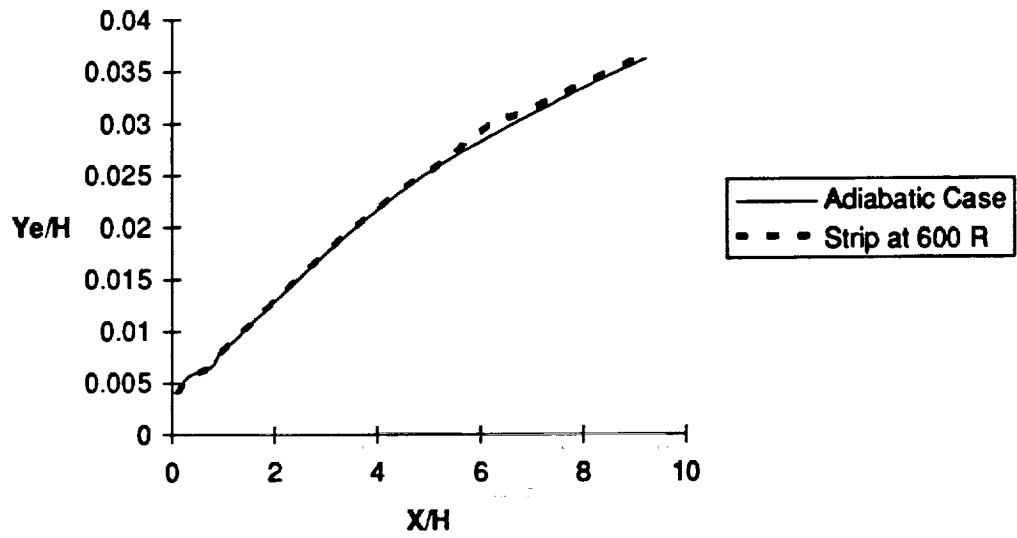
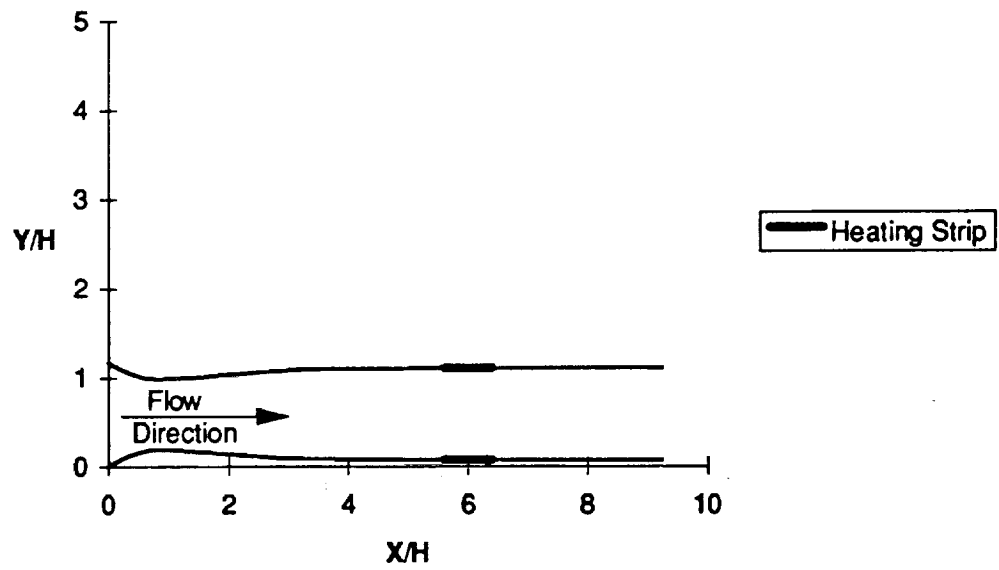


Figure 2.6 Comparison of the second derivative of velocity profiles at $X/H = 9.23$ with the Heating/Cooling Strip at $2.86 \leq X/H \leq 3.73$

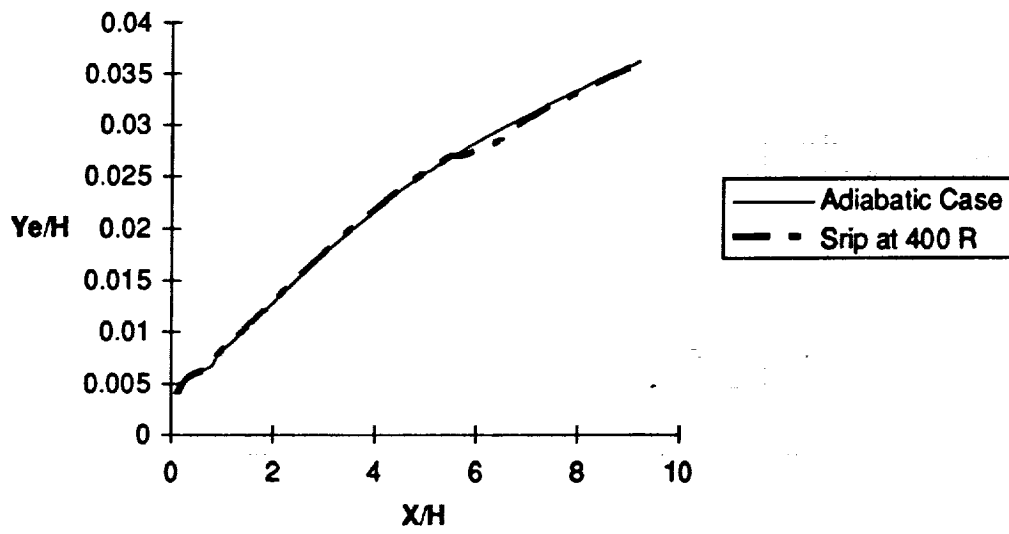


(a) Boundary Layer Growth

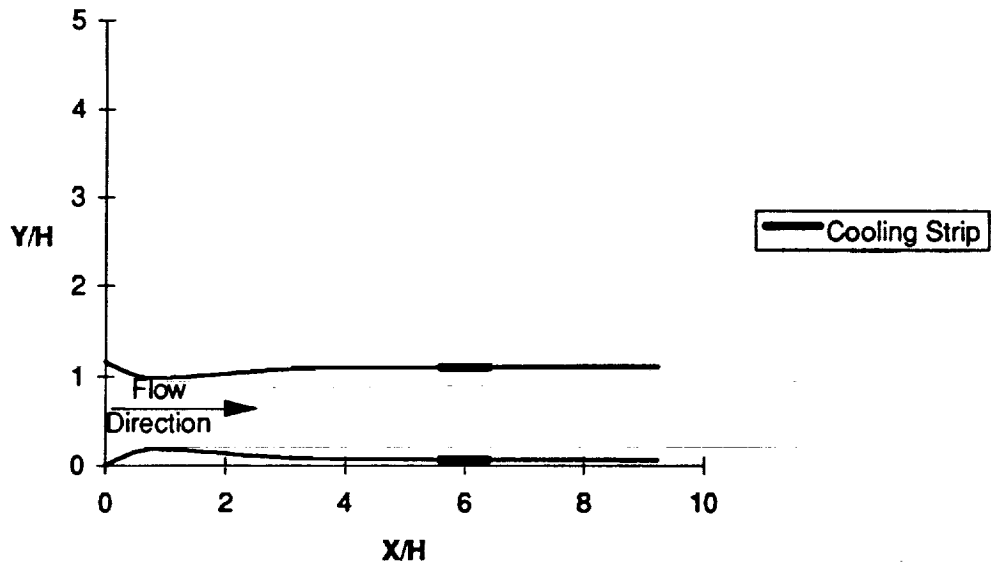


(b) PoC Nozzle and Test Section Geometry

Figure 2.7 Growth of Boundary Layer for the Adiabatic and Strip Heating Case. The location of the Heating Strip ($5.61 \leq X/H \leq 6.41$) on the nozzle wall is shown in bold



(a) Boundary Layer Growth



(b) PoC Nozzle and Test Section Geometry

Figure 2.8 Growth of Boundary Layer for the Adiabatic and Strip Cooling Case. The location of the Cooling Strip ($5.61 \leq X/H \leq 6.41$) on the nozzle wall is shown in bold

strip, are seen in Figure 2.9 and Figure 2.10 respectively. As would be expected, since these profiles are upstream of the heating/cooling strip, heating or cooling has little effect at this location ($X/H = 5.23$). However, when a downstream location is selected, the effect is appreciable. Heating at $5.61 \leq X/H \leq 6.41$ results in a more positive $\left(\frac{\partial T}{\partial y}\right)$ term and a smaller $\left(\frac{\partial^2 u}{\partial y^2}\right)$ term near the wall, as seen in Figures 2.11 and 2.12.

2.4 Summary of Results

Several observations can be made from the information in this chapter. First, the addition of heat to the boundary layer improves the stability of the boundary layer at downstream locations because at these locations, the boundary layer is hot relative to the cooler wall; thus, heat energy is transferred from the boundary layer to the wall. Second, applying cooling to the boundary layer results in lower stability of the boundary layer at downstream locations, since the downstream boundary layer is cooler than the wall and therefore produces a heating effect on the boundary layer. Third, the effect of heating and cooling on boundary layer stability decreases as the distance from the heated or cooled area becomes greater. However, the Stability Modifier Method alone provides no mechanism to account for flow instability.

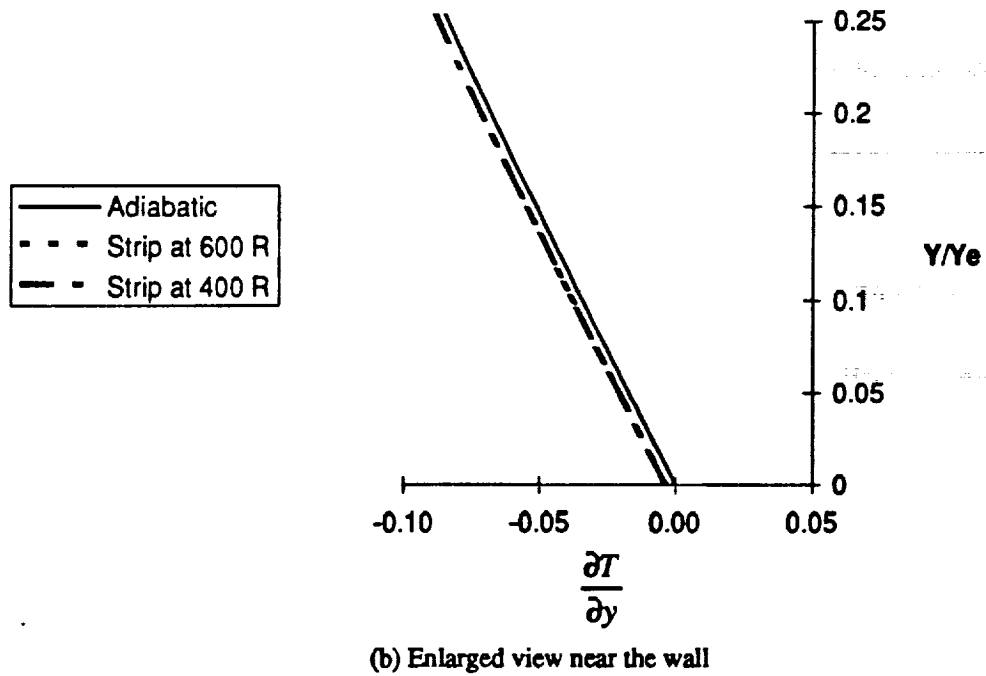
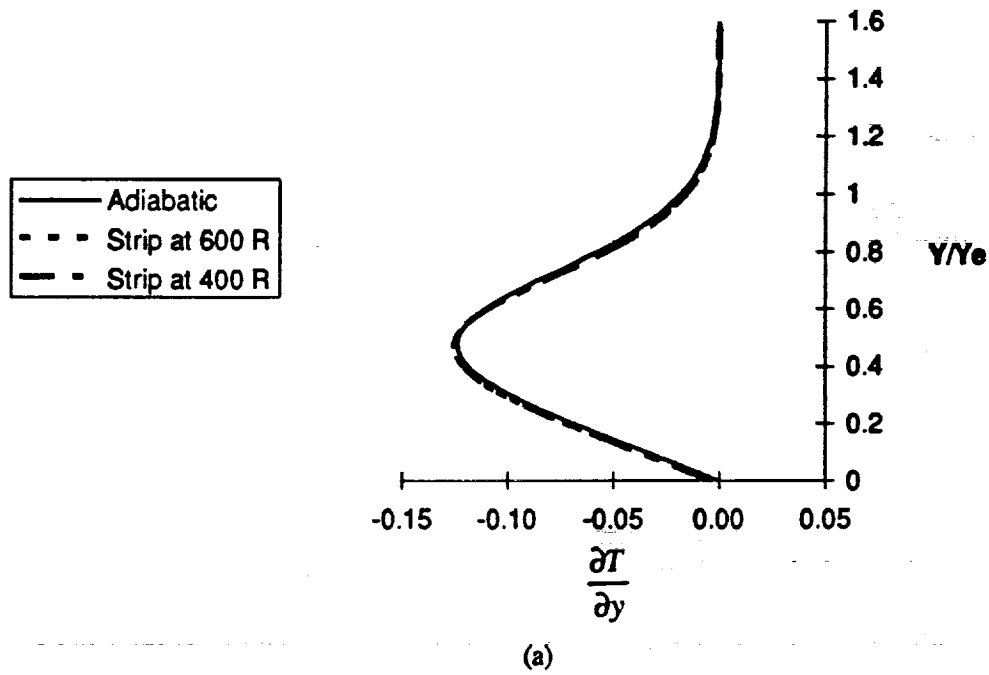
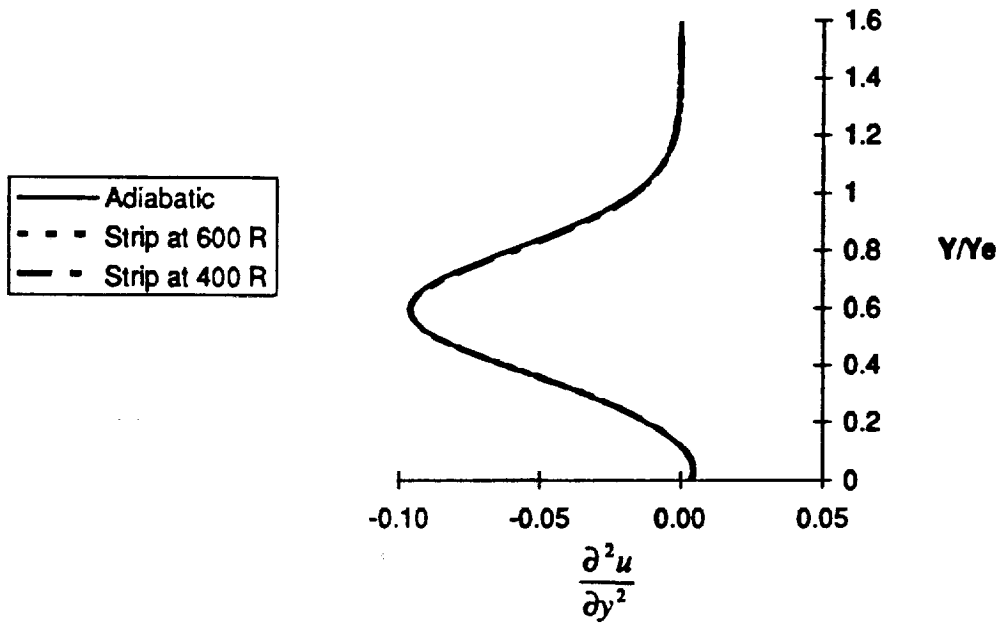
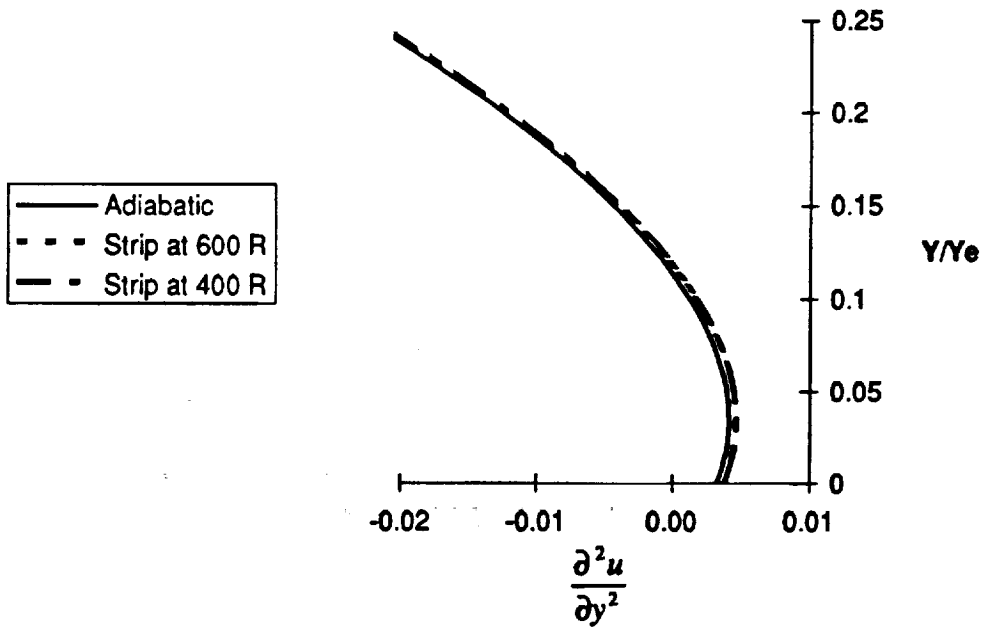


Figure 2.9 Comparison of the first derivative of temperature profiles at $X/H = 5.23$ with the Heating/Cooling Strip at $5.61 \leq X/H \leq 6.41$

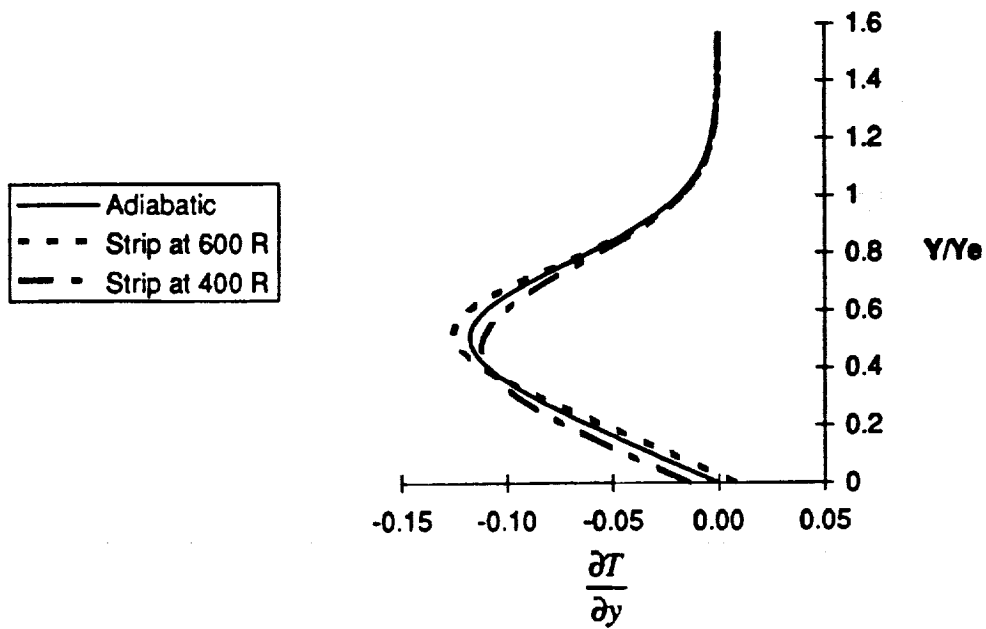


(a)

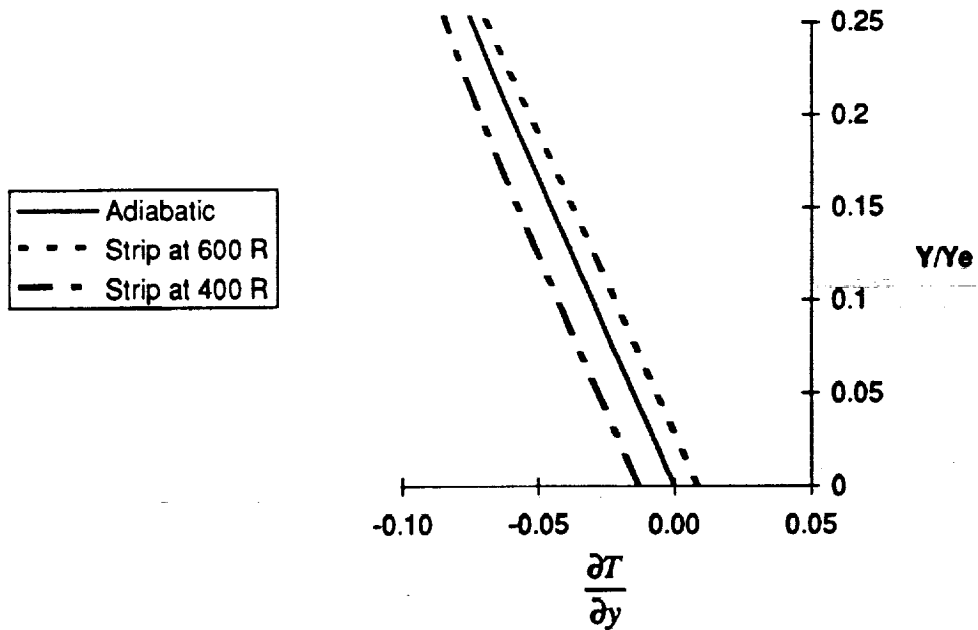


(b) Enlarged view near the wall

Figure 2.10 Comparison of the second derivative of velocity profiles at $X/H = 5.23$ with the Heating/Cooling Strip at $5.61 \leq X/H \leq 6.41$

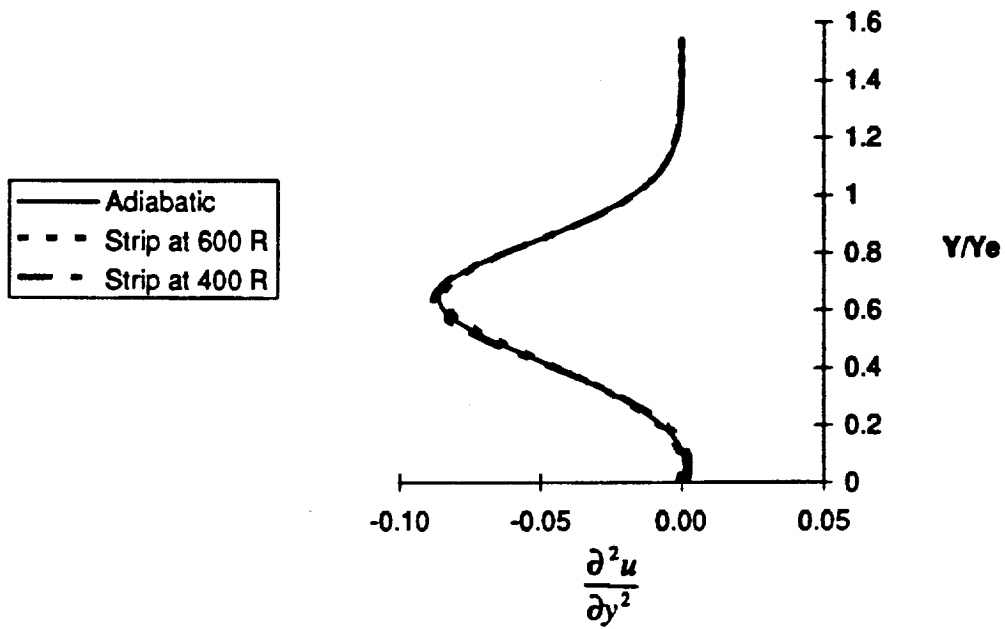


(a)

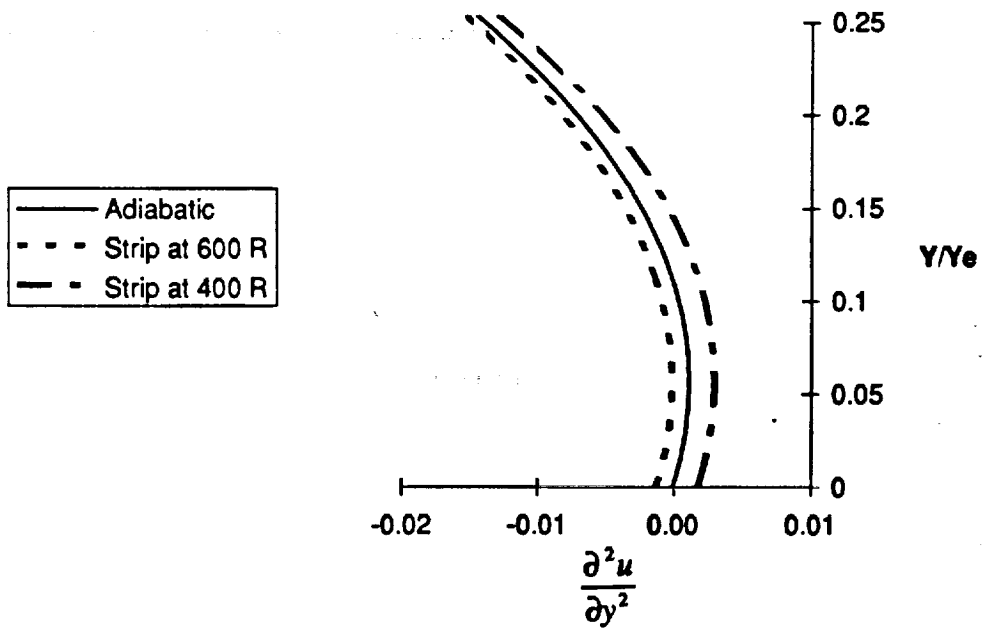


(b) Enlarged view near the wall

Figure 2.11 Comparison of the first derivative of temperature profiles at $X/H = 9.23$ with the Heating/Cooling Strip at $5.61 \leq X/H \leq 6.41$



(a)



(b) Enlarged view near the wall

Figure 2.12 Comparison of the second derivative of velocity profiles at $X/H = 9.23$ with the Heating/Cooling Strip at $5.61 \leq X/H \leq 6.41$

Chapter 3

Study of Boundary Layer Stability Using e^N Method

3.1 Summary of Compressible Linear Stability Theory and e^N Method

If we assume the basic flow is known and the flow is a function of y , the normal to the wall direction, the flow field may be depicted by the mean flow and a small amplitude harmonic wave form, for example velocity and pressure.

$$u(x,y,z,t) = \bar{u}(y) + \epsilon \hat{u}(y)e^{i(\alpha x + \beta z - \omega t)} \quad (3.1)$$

$$p(x,y,z,t) = \bar{p}(y) + \epsilon \hat{p}(y)e^{i(\alpha x + \beta z - \omega t)} \quad (3.2)$$

In the above equations, ϵ is a small value, α is the x wave number, β is the z wave number, and ω is the frequency of the disturbance. For spatial stability of two-dimensional flow, β and ω can be assumed to be real numbers with α being complex. This means that β and ω will grow if $-\alpha_i \geq 0$; therefore, α_i is the disturbance growth rate. The disturbance growth rate is used to obtain the N Factor as follows:

$$N(f) = - \int_{x_0}^x \alpha_i(x) dx \quad (3.3)$$

where the N Factor is a function of frequency and is used as the exponent in the total amplification rate (e^N).

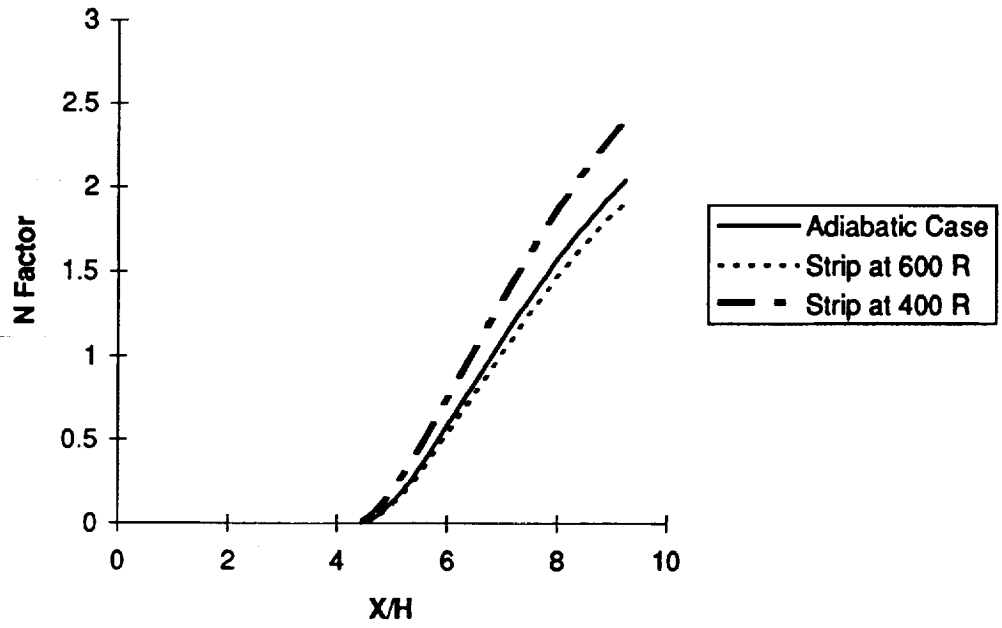
The N Factor can be used to predict the onset of transition when the N Factor reaches a value of approximately 10 if external disturbances are small. If the external disturbances are high, the value of the N Factor which initiates transition is markedly lower. There are many excellent sources of information on linear stability theory such as References 17 and 18.

3.2 Description of e^{Malik} Code

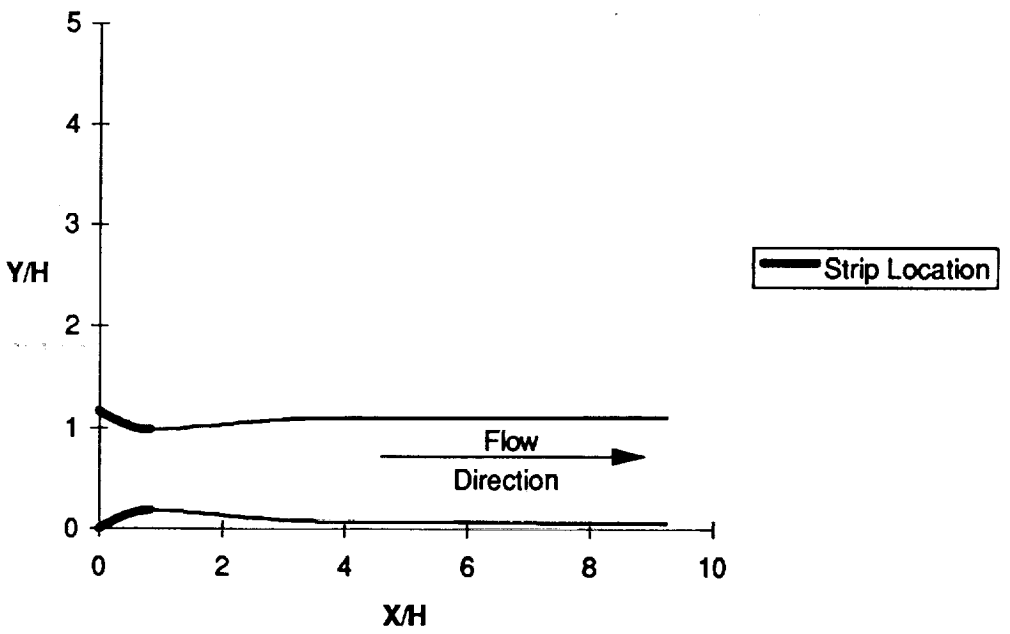
The code used in this thesis to solve the compressible linear spatial boundary layer stability problem described in Section 3.1 and to obtain the N Factor for various cases is the e^{Malik} Code (Reference 16). This code uses output from the boundary layer code, which is discussed in the previous chapter, and an input control file prepared by the writer. The output from the boundary layer code provides the necessary boundary layer flow parameters, and the input control file provides such information as the frequency of the disturbances of interest, location along the body for starting the stability calculations, and types of instability to calculate for (Tollmien-Schlichting or Görtler). The input file also allows the user to select either two-dimensional or axisymmetric flow.

3.3 Results Obtained for the PoC Wind Tunnel

In this section the effect of the location of the heating and cooling strip on the stability of the boundary layer is studied by using information obtained from the e^{Malik} code discussed in Section 3.2. For the Proof of Concept (PoC) supersonic wind tunnel at Ames Research Center, the nozzle and test section flow is two-dimensional. Also, the nozzle is comparatively long in relation to the test section height, and Tollmien-Schlichting instability is dominant over Görtler instability. Therefore, two-dimensional flow and Tollmien-Schlichting instability are selected as conditions to investigate. The heating/cooling strip is located in seven different locations. For all the cases the stagnation pressure is 10 psia, the stagnation temperature is 560°R , the test section Mach number is 1.6, and the adiabatic wall temperature is approximately 500°R . For all cases considered, the heating strip is at 600°R , and the cooling strip is at 400°R . The disturbance frequency of 14 kHz is chosen because it is observed that this frequency results in the maximum instability. Figure 3.1 shows the location of the heating/cooling strip ($0.00 \leq X/H \leq 0.84$) on the nozzle wall for the first case and the effect of both the heating and cooling strips on the N Factor growth. It also compares the N Factor growth to the adiabatic case. As seen in Figure 3.1, the cooling strip causes the N Factor to grow faster than in the adiabatic case, and the heating strip causes the N Factor to decrease. Therefore, for this first case, when the heating strip is applied, the boundary layer is more stable. The heating/cooling strip is located in six other positions, and the N Factor growth along the nozzle and test section wall is



(a) N Factor Growth



(b) Heating/Cooling Strip Location on the PoC Nozzle and Test Section

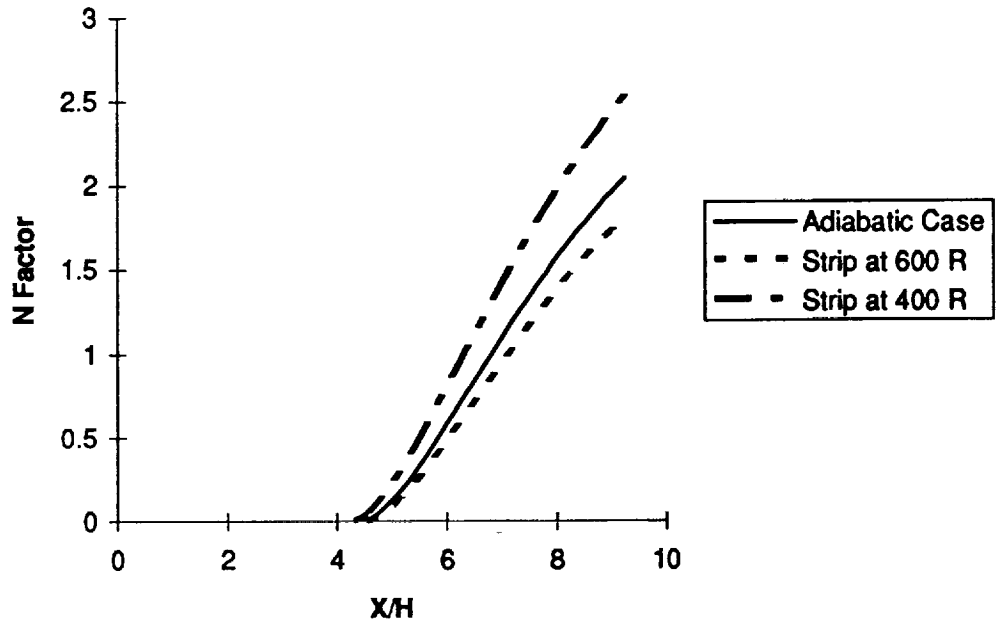
Figure 3.1 N Factor Growth with the Heating/Cooling Strip located at $0.00 \leq X/H \leq 0.84$ for a disturbance frequency of 14 kHz

obtained for each. The growth for each is then compared to the adiabatic N Factor growth.

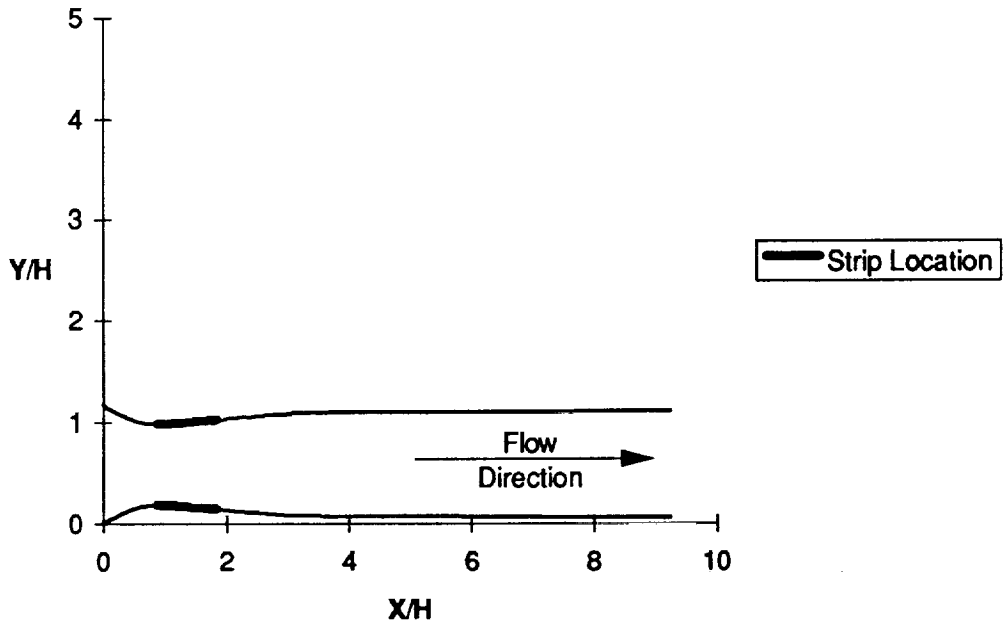
As heating/cooling is applied downstream, heating improves the stability of the boundary layer and cooling makes the boundary layer less stable until the location of the heating/cooling strip is $2.86 \leq X/H \leq 3.73$, as seen in Figures 3.1 through 3.4.

When the heating/cooling strip is located at $3.80 \leq X/H \leq 4.59$, heating causes the N Factor to grow at an upstream location and to have a greater N Factor value for the entire test section than in the adiabatic case, as seen in Figure 3.5. When cooling is applied at this same location, the N Factor does not begin to grow as far upstream as when heating is applied, but the N Factor does reach a greater value at the end of the test section (Figure 3.5). The farther the heating strip location is moved downstream ($4.67 \leq X/H \leq 5.54$ and $5.61 \leq X/H \leq 6.41$), the greater the increase is in the value of the N Factor. Thus, the stability of the boundary layer decreases, as seen in Figure 3.6 and Figure 3.7. When the cooling strip is located at $4.67 \leq X/H \leq 5.54$, the value of the N Factor is non-existent for most of the length of the nozzle and test section of the PoC Wind Tunnel, as can be seen in Figure 3.6.

Next, the cooling strip is located at $5.61 \leq X/H \leq 6.41$. At this location, the N Factor grows just as in the adiabatic case until the flow reaches the cooling strip. There the cooling strip causes a substantive decrease in the N Factor value, as seen in Figure 3.7.

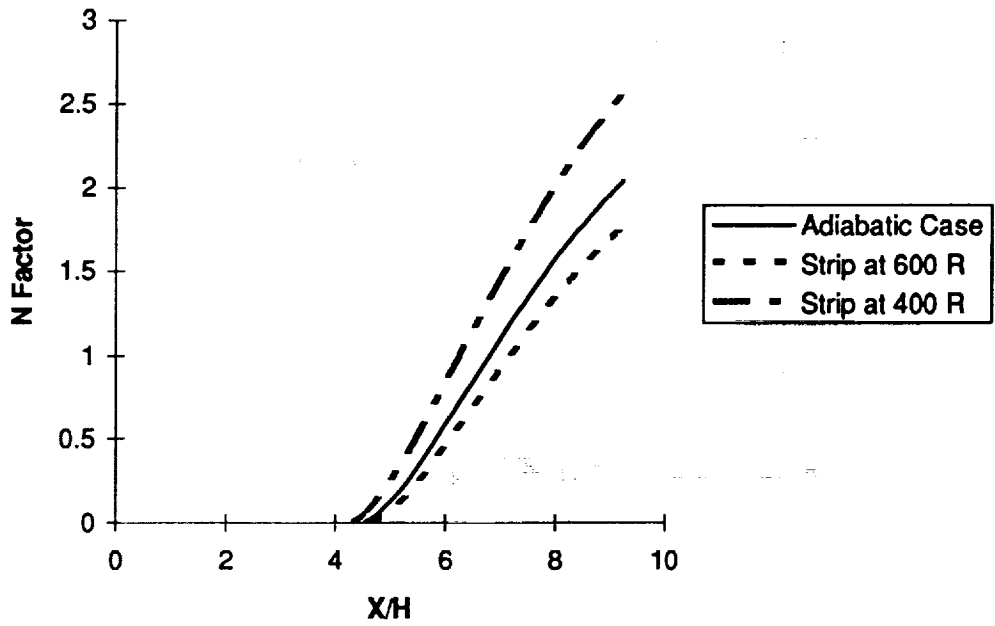


(a) N Factor Growth

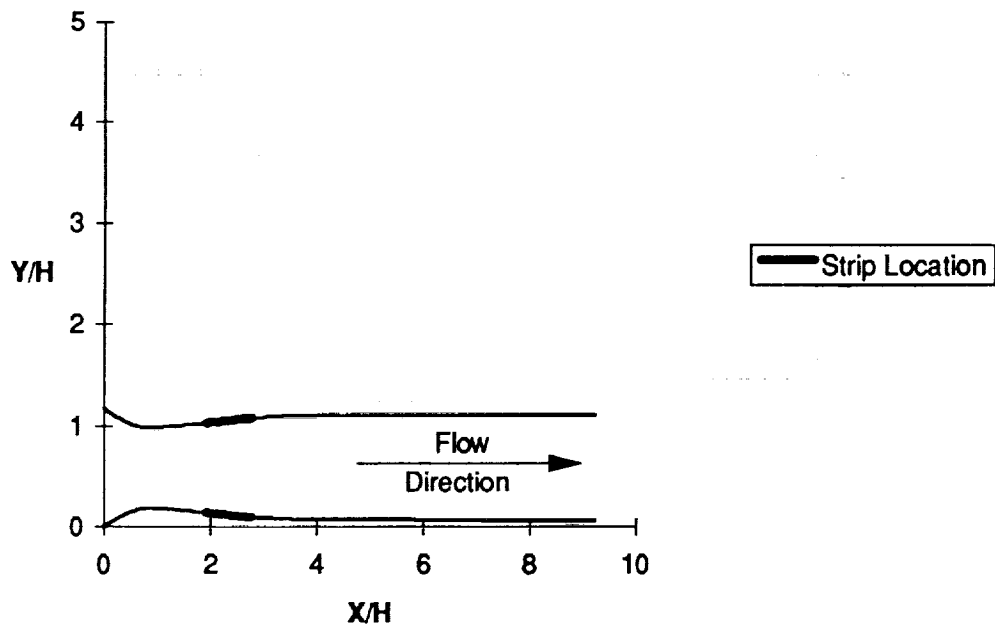


(b) Heating/Cooling Strip Location on the PoC Nozzle and Test Section

Figure 3.2 N Factor Growth with the Heating/Cooling Strip located at $0.88 \leq X/H \leq 1.85$ for a disturbance frequency of 14 kHz

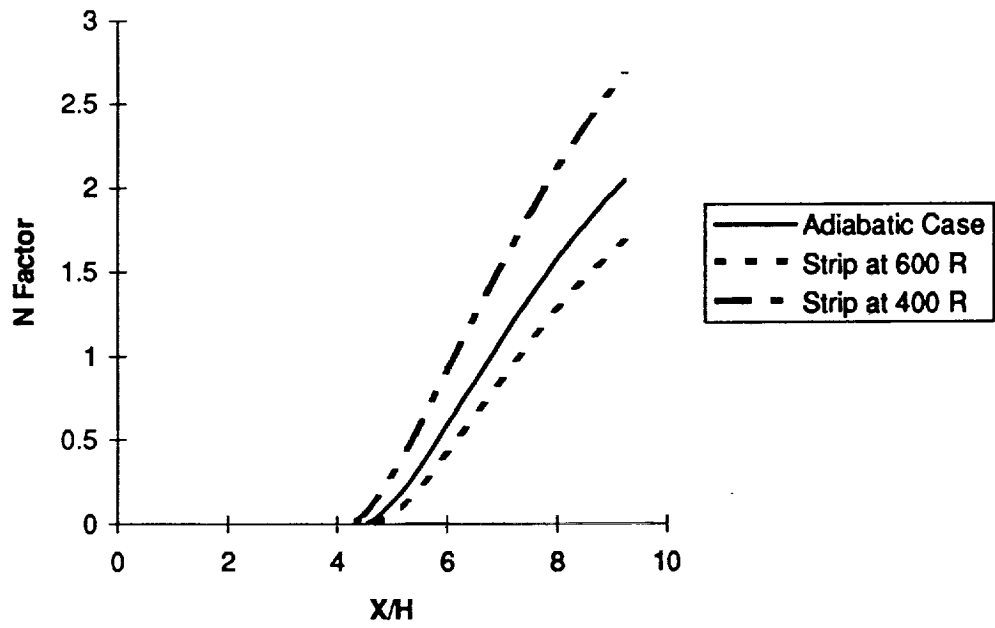


(a) N factor Growth

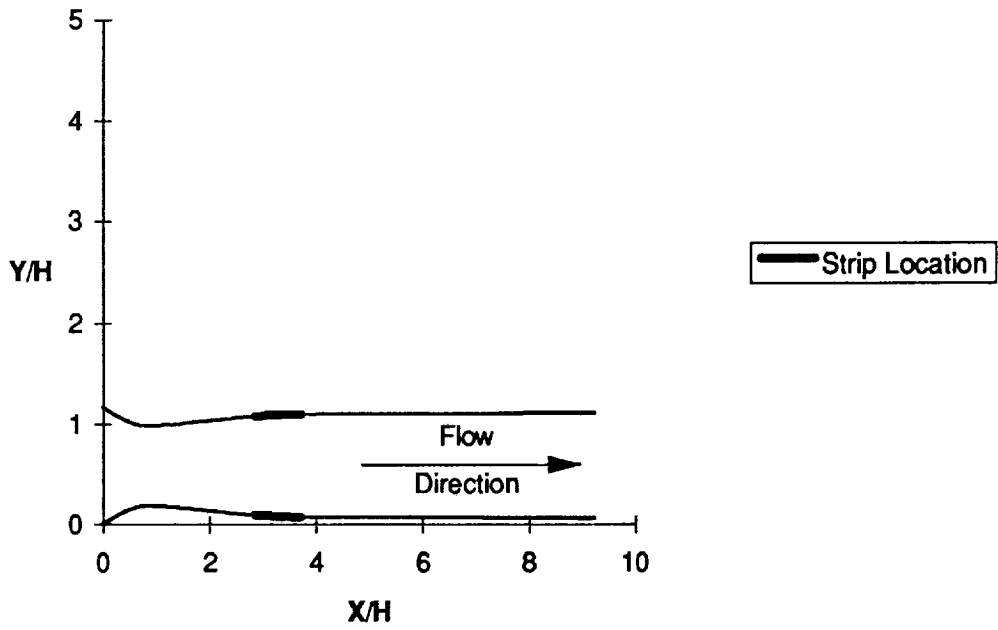


(b) Heating/Cooling Strip Location on the PoC Nozzle and Test Section

Figure 3.3 N Factor Growth with the Heating/Cooling Strip located at $1.93 \leq X/H \leq 2.78$ for a disturbance frequency of 14 kHz

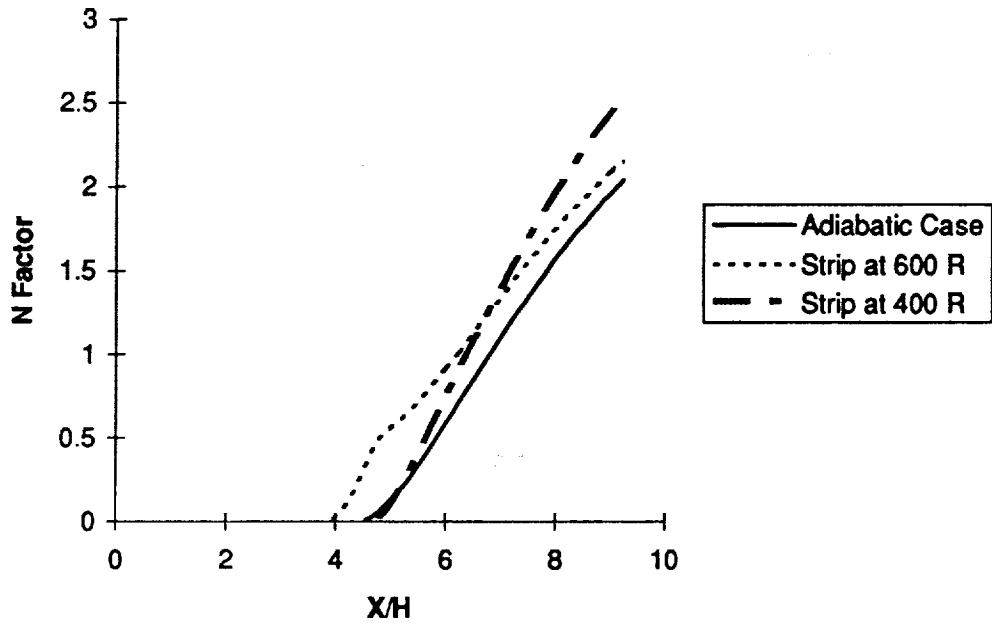


(a) N Factor Growth

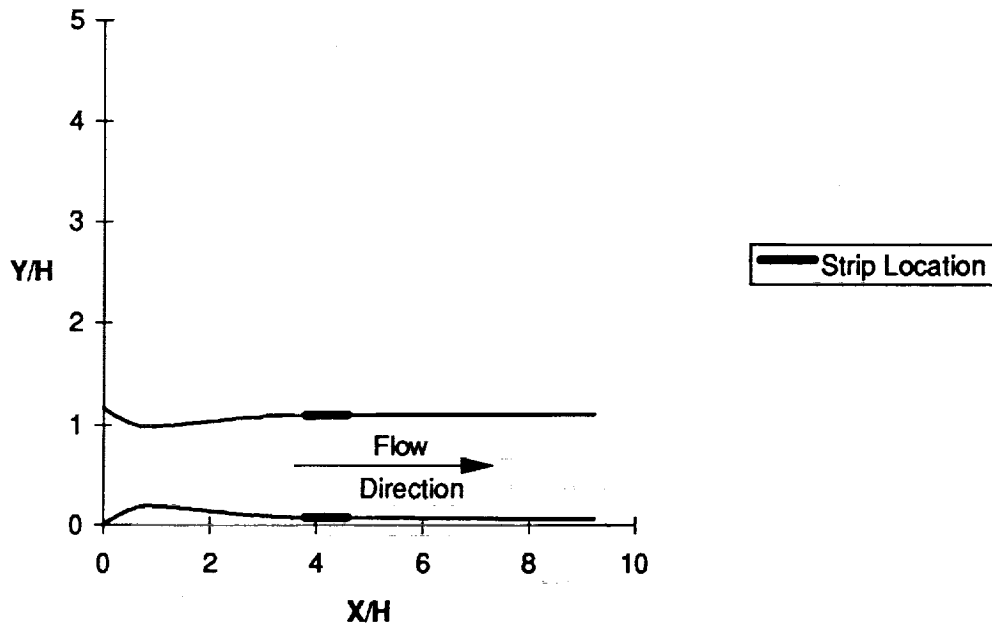


(b) Heating/Cooling Strip Location on the PoC Nozzle and Test Section

Figure 3.4 N Factor Growth with the Heating/Cooling Strip located at $2.86 \leq X \leq 3.73$ for a disturbance frequency of 14 kHz

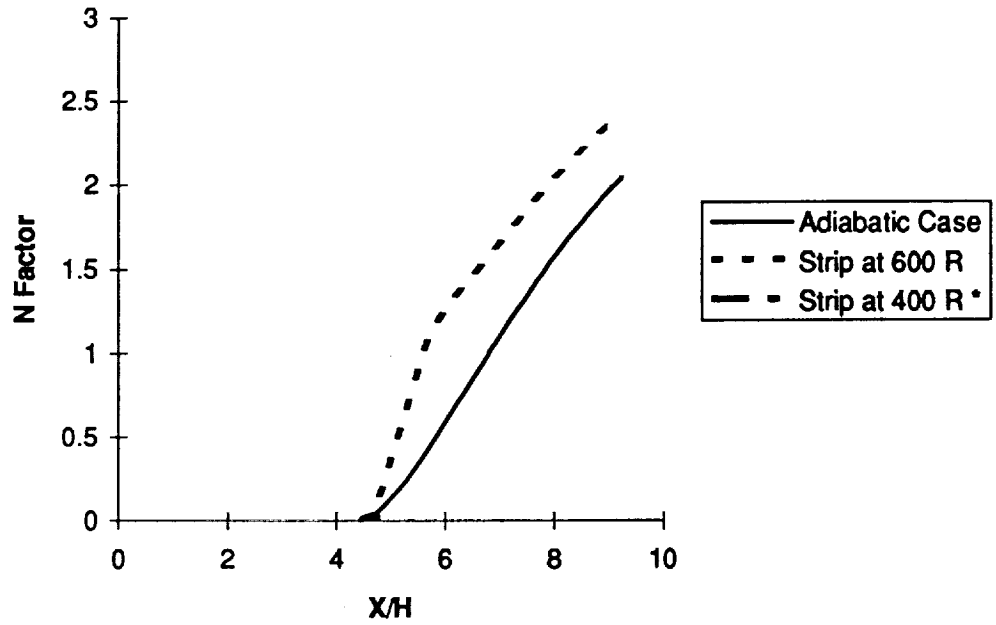


(a) N Factor Growth

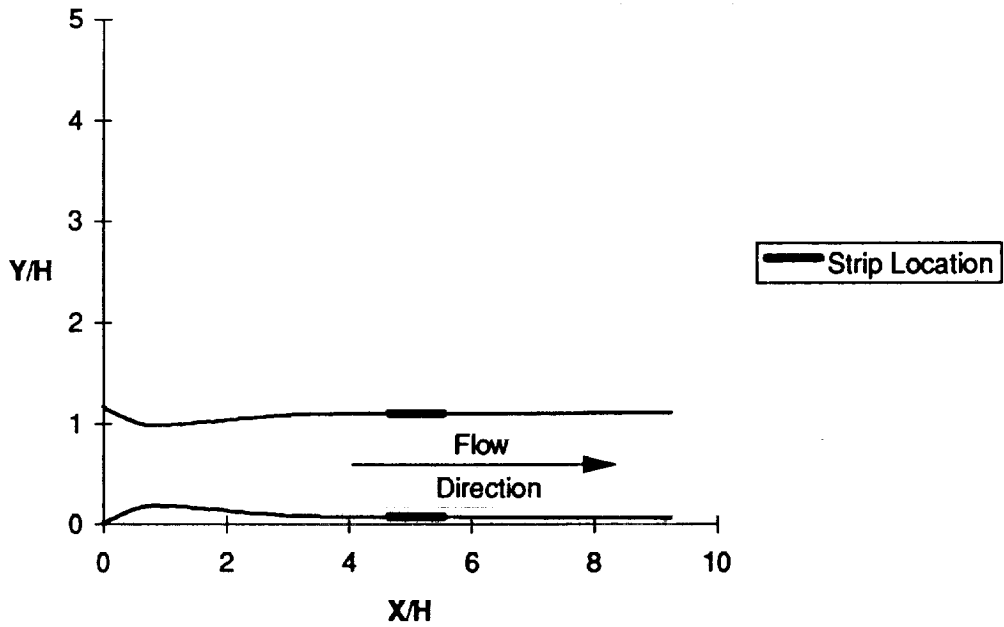


(b) Heating/Cooling Strip Location on the PoC Nozzle and Test Section

Figure 3.5 N Factor Growth with the Heating/Cooling Strip located at $3.80 \leq X/H \leq 4.59$ for a disturbance frequency of 14 kHz

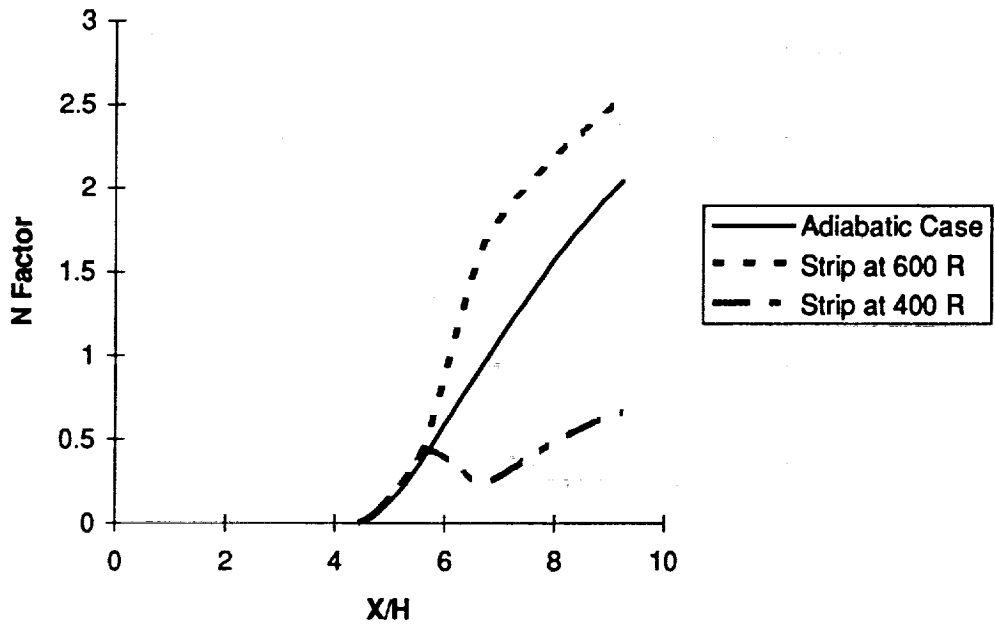


(a) N Factor Growth

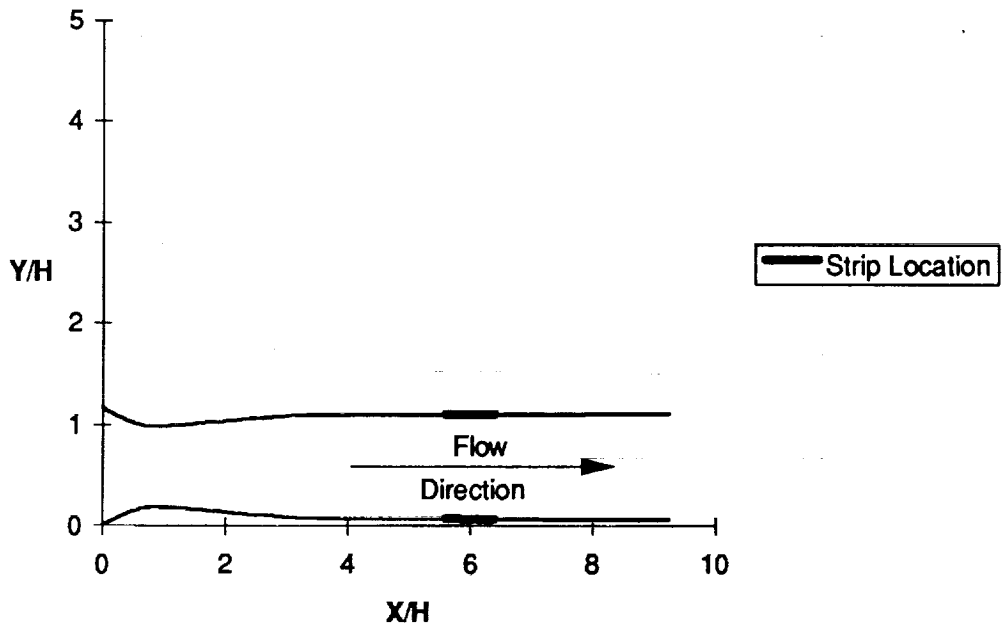


(b) Heating/Cooling Strip Location on the PoC Nozzle and Test Section

Figure 3.6 N Factor Growth with the Heating/Cooling Strip located at $4.67 \leq X/H \leq 5.54$ for a disturbance frequency of 14 kHz *N Factor is too small to be seen for this case



(a) N Factor Growth



(b) Heating/Cooling Strip Location on the PoC Nozzle and Test Section

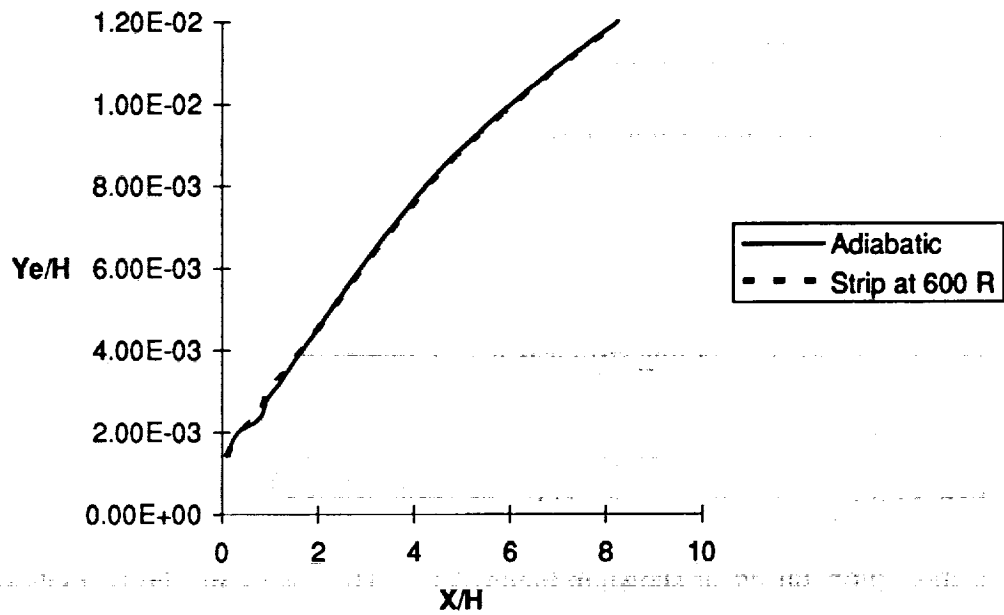
Figure 3.7 N Factor Growth with the Heating/Cooling Strip located at $5.61 \leq X/H \leq 6.41$ for a disturbance frequency of 14 kHz

3.4 LFSWT Results

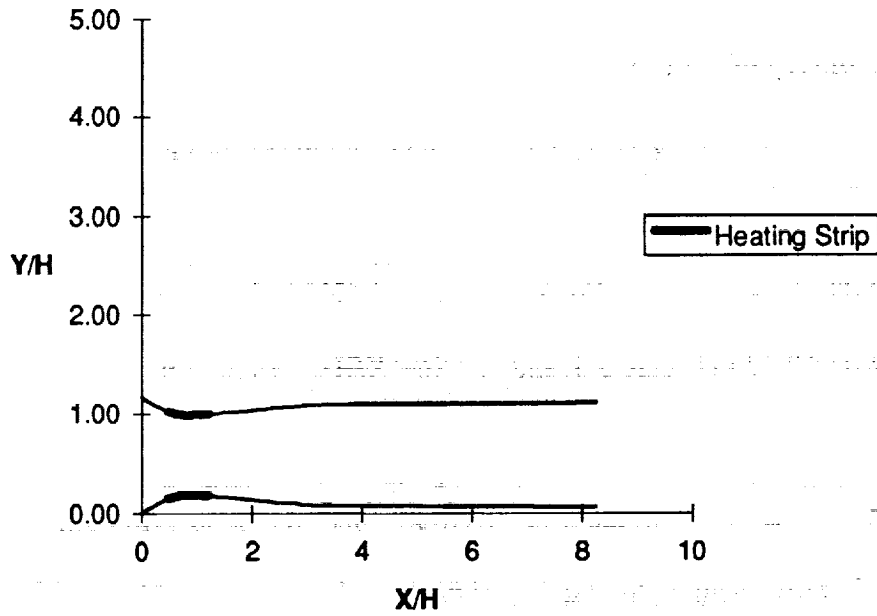
For the LFSWT, the disturbance frequency of 3000 Hz is selected, since that frequency results in maximum instability. A six-inch heating strip is located at $0.32 \leq X/H \leq 0.82$ on the nozzle of the Laminar Flow Supersonic Wind Tunnel (LFSWT). Its effect on the boundary layer thickness is relatively small, as seen in Figure 3.8. Also, a cooling strip is placed at that same location, and its effects on the boundary layer growth is also small, as seen in Figure 3.9. However, the effects of both heating and cooling on the N Factor value along the nozzle and test section wall is more pronounced, as shown in Figure 3.10. The results are similar to those obtained from the PoC Wind Tunnel discussed in Section 3.3

3.5 Summary of Results

When the heating strip is located at certain distances upstream from the beginning of the N Factor growth for the adiabatic case, for example, at $0.00 \leq X/H \leq 0.84$ as seen in Figure 3.1, at $0.88 \leq X/H \leq 1.85$ in Figure 3.2, at $1.93 \leq X/H \leq 2.78$ in Figure 3.3, and at $2.86 \leq X/H \leq 3.73$ in Figure 3.4, the N Factor begins to decrease, and the stability of the boundary layer improves as compared to the adiabatic case. When the heating strip is located at $2.86 \leq X/H \leq 3.73$, the greatest improvement in the stability of the boundary layer is achieved. When the heating strip is located just upstream of the beginning of the N Factor growth for the adiabatic case ($3.80 \leq X/H \leq 4.59$), the heating strip causes the N Factor value to

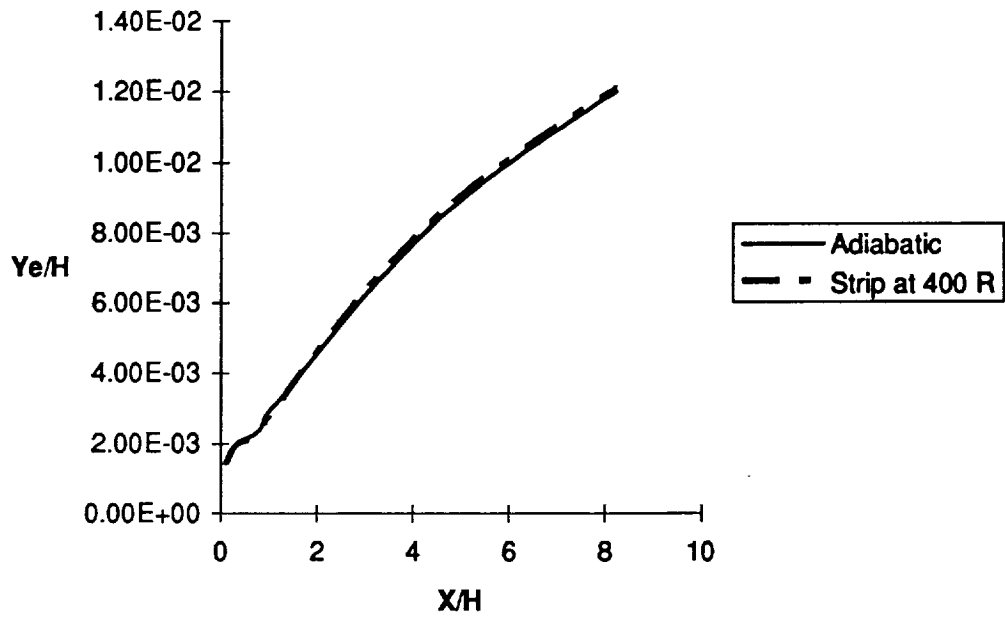


(a) Boundary Layer Growth

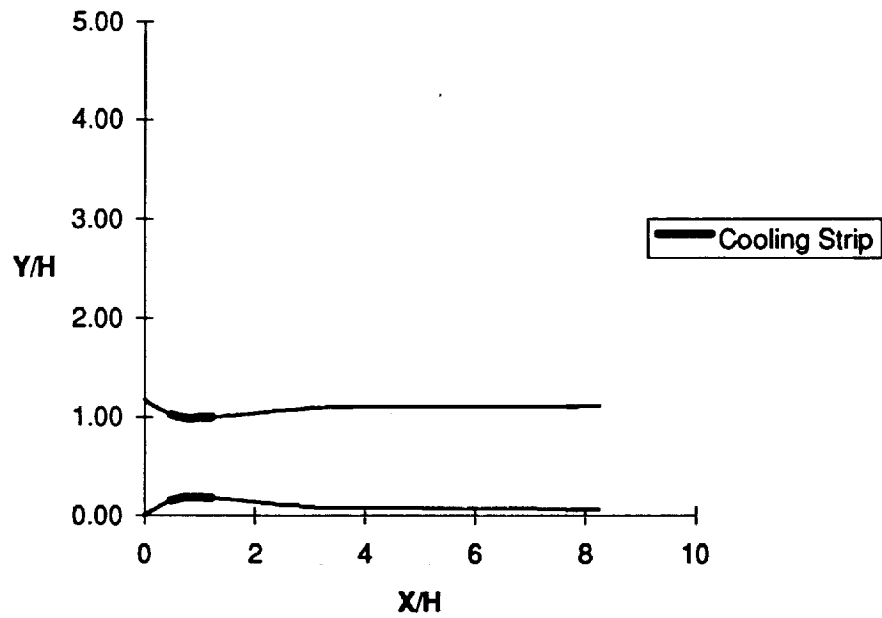


(b) Location of the Heating Strip on the LFSWT Nozzle

Figure 3.8 Comparison of Boundary Layer growth for the Adiabatic case and the case where the Heating Strip is located at $0.48 \leq X/H \leq 1.23$ on the nozzle of the LFSWT

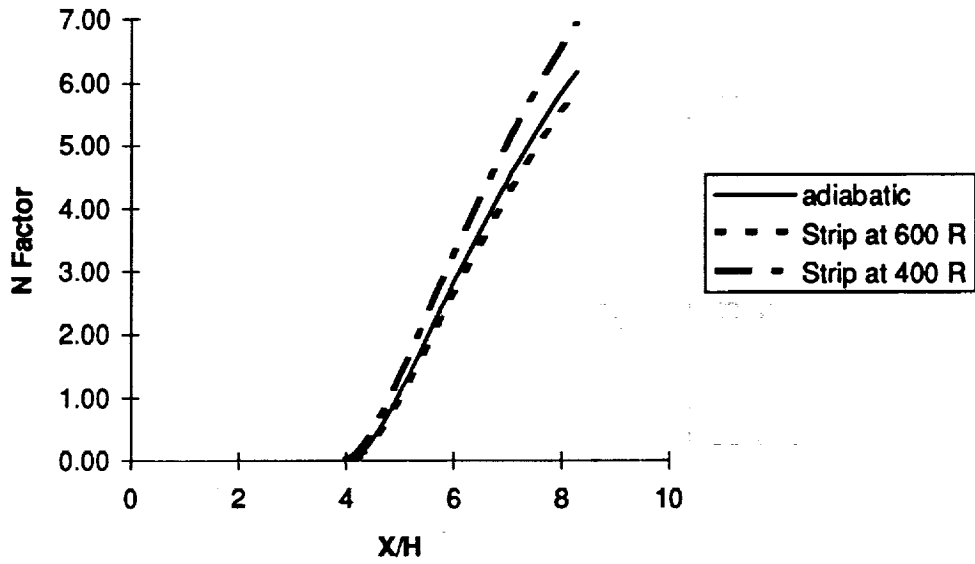


(a) Boundary Layer Growth

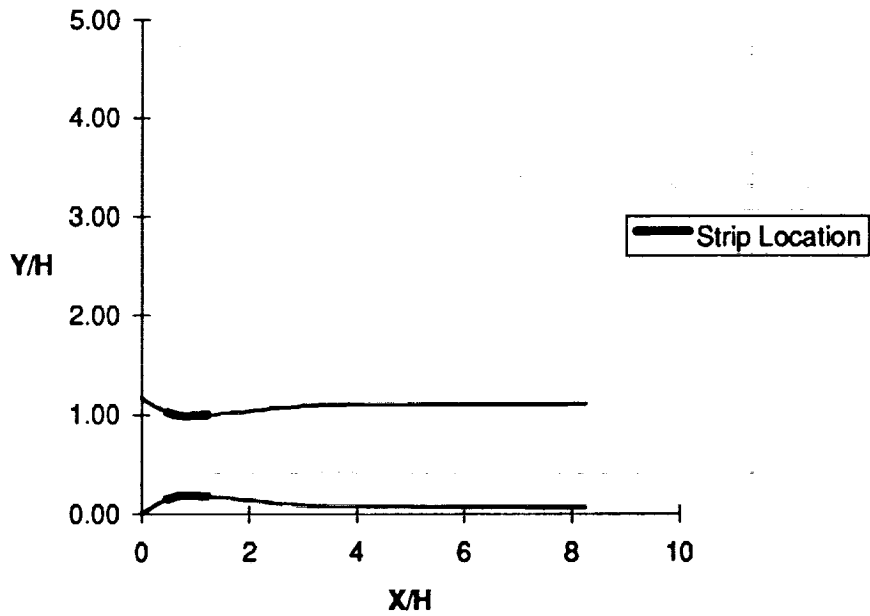


(b) Location the Cooling Strip of the LFSWT Nozzle

Figure 3.9 Comparison of Boundary Layer growth for the Adiabatic case and the case where the Cooling Strip is located at $0.48 \leq X/H \leq 1.23$ on the nozzle of the LFSWT



(a) N Factor Growth



(b) Location of the Heating/Cooling Strip on the LFSWT Nozzle

Figure 3.10 N Factor growth for the Adiabatic case, case where the Heating Strip is located at $0.48 \leq X/H \leq 1.23$ and the case where the Cooling Strip is located at $0.48 \leq X/H \leq 1.23$ for the LFSWT. Frequency = 3000 Hz

increase in comparison to the N Factor for the adiabatic case (Figure 3.5), thus causing the boundary layer to become less stable. For the cases where the heating strip is located farther downstream ($4.67 \leq X/H \leq 5.54$ and $5.61 \leq X/H \leq 6.41$), the boundary layer becomes less stable, as seen in Figure 3.6 and Figure 3.7. Therefore, at these locations, any benefit from the cooling effect downstream of the heating strip is negated because the instability has already begun and the heating strip causes the instability to grow even more. Applying heat at the $0.32 \leq X/H \leq 0.82$ location on the LFSWT nozzle causes the N Factor at the exit of the test section to decrease to 5.87 as compared to 6.17 for the adiabatic case.

Locating the cooling strip upstream of the beginning of the N Factor growth has a destabilizing effect on the boundary layer as seen in Figures 3.1 through 3.5, with the highest value for the N Factor occurring when the cooling strip is located at $2.86 \leq X/H \leq 3.73$, as seen in Figure 3.4. At this same location, the heating strip has the greatest effect on stabilization of the boundary layer. Almost complete elimination of any instability can be achieved in the output of the code when the cooling strip is located at $4.67 \leq X/H \leq 5.54$, as seen in Figure 3.6. With the cooling strip at $5.61 \leq X/H \leq 6.41$, the N Factor is greatly reduced (and stabilization is increased) over the adiabatic case as seen in Figure 3.7. Applying cooling at the $0.32 \leq X/H \leq 0.82$ location on the LFSWT nozzle causes the N Factor at the exit of the test section to increase to 6.93 as compared to 6.17 for the adiabatic case.

Chapter 4

Conclusions and Recommendations

4.1 Conclusions

The purpose of this study is to gain an insight into the effects of applying heating and cooling strips on the boundary layer stability of the Proof of Concept (PoC) Wind Tunnel and Laminar Flow Supersonic Wind Tunnel (LFSWT). The two different methods used in this study are the Stability Modifier Method (Chapter 2) and the e^N Method using Linear Stability Theory (Chapter 3). The two different CFD codes used to carry out this study are the boundary layer code (Reference 15) and the e^{Malik} code, which is a Spatial Linear Stability code using the e^N Method (Reference 16).

The two methods used in Chapter 2 (Stability Modifier Method) and Chapter 3 (e^N Method) demonstrate that heating upstream of the location where instability begins improves the boundary layer stability and that cooling upstream of that location destabilizes the boundary layer in both the PoC Wind Tunnel and the LFSWT. The e^N Method indicates that heating downstream of the location where instability begins results in the boundary layer's becoming more unstable and that cooling downstream at this location improves the stability of the boundary layer. But the results obtained from the Stability Modifier Method show the same effect whether the

heating/cooling strip is applied upstream or downstream of the location where instability starts. That is, heating upstream improves the stability of the boundary layer downstream, and cooling upstream decreases the stability of the boundary layer.

Therefore, to obtain greater stability, heating should be applied upstream of the location of the beginning of instability, and if cooling is applied, it should be located near the point of beginning instability or downstream of the point where actual instability starts. These results are consistent with the findings for a flat plate with subsonic flow of Masad and Nayfeh (Reference 12) and for flat plates and nozzles at supersonic Mach number of Lafrance (Reference 13). Also, Demetriades' experimentation found that heating delays transition on the nozzle of a supersonic wind tunnel (Reference 11) and that cooling accelerates transition on the nozzle (Reference 12). For actual tunnel runs, nozzle surface roughness, stilling chamber disturbances, outside wall vibration, etc. cause the beginning point of actual instability to be upstream of the location predicted in this study.

Although this is a qualitative study of the effect on the boundary layers of heating and cooling the walls of the nozzles and test section of the PoC Wind Tunnel and the LFSWT, the codes can be used to model actual experiments of these effects. Also, studies of this type can be used to aid in the development of aircraft where laminar flow control is important.

4.2 Recommendations

It is recommended that further study of the effect of heating and cooling on boundary layer stability be systematically carried out on the LFSWT. Particular attention should be paid to when the cooling strip is located at the point of the on-set of instability to determine the validity of the results obtained from this study. Also, further study is needed, since the changes in thickness of the boundary layer, which are the results of heating and cooling, can cause disturbances in the tunnel's free-stream flow.

When experiments of these effects are conducted in the wind tunnels, the methods and codes used in this study should be used to model the temperature distribution of the actual experiment.

List of References

List of References

1. Wolf, S. W. D., Laub, J. A., King, L. S., and Reda, D. C.; "Development of the NASA Ames Low-Disturbance Supersonic Wind Tunnel for Transition Research Up to Mach 2.5," AIAA Paper No. 92-2909, July 1992.
2. Pate, S. R.; "Dominance of Radiated Aerodynamic Noise on Boundary-Layer Transition in Supersonic-Hypersonic Wind Tunnels: Theory and Application," Ph.D. Dissertation, University of Tennessee, March 1977.
3. Kovasznay, L. S. G.; "Turbulence In Supersonic Flow," *Journal of the Aeronautical Sciences*, Vol. 20, No. 10, October 1953, pp. 657-674.
4. Laufer, J.; "Aerodynamic Noise in Supersonic Wind Tunnels," *Journal of Aerospace Sciences*, Vol. 28, No. 9, September 1961, pp. 685-692.
5. Pate, S. R., and Schueler, C. J., "Radiated Aerodynamic Noise Effects on Boundary Layer Transition in Supersonic and Hypersonic Wind Tunnels," *AIAA Journal*, Vol. 7, No. 3, March 1969, pp. 685-692.
6. Beckwith, I., Chen, S., Wilkinson, S., Malik, M., and Tuttle, D.; "Design and Operational Features of Low Disturbance Wind Tunnels at NASA Langley for Mach Number from 3.5 to 18," AIAA Paper No. 90-1391, June 1990.
7. Chen, F.-J., Malik, M. R., and Beckwith, I. E.; "Boundary-Layer Transition on a Cone and Flat Plate at Mach 3.5," *AIAA Journal*, Vol. 27, No. 6, June 1989.
8. Chen, F.-J., Beckwith, I. E., and Creel, T. R., Jr.; "Correlations of Supersonic Boundary-Layer Transition on Cones Including Effects of Large Axial Variations in Wind-Tunnel Noise," NASA Technical Paper 2229, January 1984.
9. Pate, S. R.; "Effects of Wind Tunnel Disturbances on Boundary-Layer Transition with Emphasis on Radiated Noise: A Review," AIAA Paper No. 80-0431, March 1980.
10. Demetriades, A.; "Stabilization of a Nozzle Boundary Layer by Surface Heating," AIAA Paper No. 94-2501, June 1994.

11. Demetriades, A.; "Cooling and Roughness Effects on Transition on Nozzle Throats and Blunt Bodies," *Journal of Spacecraft and Rockets*, Vol. 29, No. 4, July-August 1992,
12. Masad, J. A., and Nayfeh, A. H.; "Laminar flow control of subsonic boundary layers by suction and heat-transfer strips," *Physics of Fluids*, June 1992, pp. 1259-1272.
13. Lafrance, R.; "Stability Study of Laminar Boundary Layers with Wall Temperature Effects Using Numerical Methods," M. S. Thesis, University of Tennessee, August 1994.
14. Reshotko, E.; "Stability and Transition, How Much Do We Know?," *Proceedings of the Tenth U.S. National Congress of Applied Mechanics*, ASME, New York, 1987, pp. 412-434.
15. Harris, J. E., and Blanchard, D. K.; "Computer Program for Solving Laminar, Transitional, or Turbulent Boundary Layer Equations for Two-Dimensional and Axisymmetric Flow," NASA TM 83207, February 1982.
16. Malik, M. R.; "e^{Malik}: A New Spatial Stability Analysis Program for Transition Prediction Using the e^N Method," High Technology Corporation, Report No. HTC-8902, March 1989.
17. Mack, L. M.; "Boundary Layer Linear Stability Theory," *Special Course on Stability and Transition of Laminar Flow*, Von Karman Institute, AGARD-R-709, March 1984.
18. White, F. M.; *Viscous Flow*, McGraw-Hill Inc.; New York, Second Edition, Copyright 1991.

Bibliography

Bibliography

Anderson, J. D., Jr.; *Modern Compressible Flow With Historical Perspective*, Second Edition, McGraw-Hill, Inc., New York, 1990.

Bushnell, D. M., Hefner, J. N.; editors, *Viscous Drag Reduction in Boundary Layers*, Volume 123, Progress in Astronautics and Aeronautics, American Institute of Aeronautics and Astronautics, Inc., Washington, DC, 1990.

John, J. E. A.; *Gas Dynamics*, Second Edition, Allyn and Bacon, Inc., Boston, Massachusetts, 1984.

Liepmann, H. W., Roshko, A.; *Elements of Gas Dynamics*, John Wiley and Sons, Inc., New York, 1957.

Schlichting, H.; *Boundary Layer Theory*, Sixth Edition, McGraw-Hill, Inc., New York, 1968.

White, F. M.; *Viscous Fluid Flow*, Second Edition, McGraw-Hill, Inc., New York, 1991.

White, F. M.; *Fluid Mechanics*, Second Edition, McGraw-Hill, inc., New York, 1986.

Vita

William Scott Meredith was born in [REDACTED].

He grew up in Winchester, Tennessee, and attended public schools there. He graduated from Franklin County High School in June, 1986, and in September, 1986, entered the University of Tennessee, Knoxville to pursue a degree in Mechanical Engineering, where he received a Bachelor of Science degree in December, 1990. He received a Master of Science degree in Mechanical Engineering from the University of Tennessee Space Institute in December, 1994.

